



Ollscoil Chathair
Bhaile Átha Cliath
Dublin City University

Development Towards a Complete, Portable Analytical System for the Detection of Phosphate in Freshwater Systems

Rachel Bracker BSc., MSc.

Thesis Presented for the Award of

Master of Science

School of Chemical Sciences

Dublin City University

Supervisors:

Prof Blánaid White, Prof Fiona Regan, & Dr. Nigel Kent

Submitted: 01/2024

Declaration

I hereby certify that this material, which I now submit for assessment on the programme of study leading to the award of Master of Science is entirely my own work, and that I have exercised reasonable care to ensure that the work is original, and does not to the best of my knowledge breach any law of copyright, and has not been taken from the work of others save and to the extent that such work has been cited and acknowledged within the text of my work.

Signed: Rachel Bracker

ID No.: 21269507

Date: 20/1/2024

Table of Contents

I List of Figures	iii
II List of Tables	vii
III Abbreviations	viii
IV Acknowledgements	1
V Abstract	1
Chapter 1: Introduction	1
1.1 Background	2
1.2 Climate Change and Effects on Phosphorus in the Environment	4
1.3 Legislation	9
1.4 Current Methods	10
1.4.1. Laboratory Methods	11
1.4.2. New Monitoring Approaches	13
1.5 Conclusions	18
1.6 Aims and Objectives	18
Chapter 2: Materials, Methods, and Development of the PhosphaSense_MiniS_D1 and PhosphaSense_MacroS_D2 Phosphate Detection Systems	20
2.1 Introduction, Aims, and Objectives	21
2.2 Reagents	21
2.3 Materials	22
2.4 Instrumentation	23
2.5 Software	23
2.5 Phosphaload diode system and its capabilities/limitations	23
2.6 Optical system redesign Part 1: PhosphaSense_MiniS_D1	25
2.7 Disc optimization	28
2.7.1 – Disc Design Process	29
2.7.2 – Layers of a Disc	31
2.7.3 – Disc Design Iterations	32
2.8 Optical system redesign Part 2: PhosphaSense_MicroS_D2	43
2.9 PhosphaSense Complete analytical system – Improvements on the Phosphaload System	44

2.10 Description of operating procedures for PhosphaSense Complete	46
2.10.1 Sample Preparation and Deployment on Disc	46
2.10.2 – PhosphaSense System Customization Options	47
2.10.3 – Analysing a Disc	48
2.11 Conclusion	50
Chapter 3: Evaluation of the PhosphaSense_MicroS_D2 System for Multisite, Phosphate Catchment Monitoring	51
3.1 Introduction	52
3.2. Aims and Objectives	52
3.3 Molybdenum Blue Method (solution and dried)	53
3.3.1 – Theory behind the Molybdenum Blue Method	53
3.3.2 – Molybdenum Blue Solution Method	55
3.3.3 – Dried Molybdenum Blue Method	55
3.4 Lab-based validation data for PhosphaSense Complete	56
3.4.1 – Validation of PhosphaSense_MiniS_D1	56
3.4.2 – Validation of PhosphaSense_MicroS_D2	58
3.5 Determination of LOD and LOQ	60
3.6 Description of Field Sites	61
3.7 Field testing results	64
3.8 Conclusion	68
Chapter 4: Overall Conclusions	69
4.1 Conclusion	70
4.2 Future Work	71
5.0 References	72
Appendix 1: List of Poster and Oral Presentations	77
A2.1. System Layout:	78
A2.2 LED screen options	79
A2.3 Analysing samples	84
A2.4 Data	88
A2.5 Other System Customizations	89

I List of Figures

Figure 1: Chart demonstrating the P trends in European lakes and rivers. It shows two time series covering 38 EEA member countries. ⁴	3
Figure 2: A visual representation of the P cycle as P moves through the environment. ¹³⁷	
Figure 3: Average Rainfall over 70 years in Ireland ²⁰	8
Figure 4: Examples of portable phosphate detection systems. From left to right: UviLux Tryptophan ³⁷ fluorescence spectrometer, PhosphaLoad ⁵ , automatic phosphate sensor developed by Lin et al. ³⁸ , Phosphate Test Strips from Precision Laboratories ³⁹	13
Figure 5: Timeline of microfluidic system for phosphate development. The iterations of the system developed for this thesis are the PhosphoSense_MicroS_D1 and PhosphaSense_MiniS_D2 (outlined in red).	19
Figure 6: (A) Phosphaload_D-PD-2021 disc, actuator, and LED-Photodiode detector. (B) 1st generation diode/photodiode head. Equipped with OSRAM Opto Semi-conductor LED and 880 nm Silicon Photosensor Photodiode ⁴³	24
Figure 7: PhosphaSense_MiniS_D1 – Dimensions: 12.5 cm tall X 7 cm diameter. Components: 880 nm IR-LED, Teensy Control Board, and a C143834MA-01 Mini-spectrometer. Casing was 3D printed using ABS.	27
Figure 8: Flow chart outlining the steps of the microfluidic disc manufacturing process from design to final assembly.	28
Figure 9: Sections of the microfluidic disc design (1) disc base, (2) spindle mounting point, (3) holes for securing disc to the spindle, (4) microfluidic channel, (5) assembly marker.	29
Figure 10: Blue layers are PMMA plastic, the top and bottom layers are 0.5 mm and the middle layer is 3 mm PMMA. The green layers are pressure sensitive adhesive (PSA) used to create the microchannels and bind each layer together.	32
Figure 11: Microfluidic disc design by Joyce O’Grady for Phosphaload_D-PD_2021. 6 sample wells; sample volume 600 µL; detection system: horizontal diode/photodiode.	33
Figure 12: Disc design 1. 8 sample wells with sample volume of 500 µL. Dimensions for areas marked above: (A) 10.4142 mm (B) 10.6744 mm (C) 6.2795 (D) 11.9174 mm (E) 1.8147 mm (F) Ø 13.2310 mm (G) 9.7888 mm (H) 3.3336 mm (I) 15.7945 mm (J) 4.000 mm (Disc diameter) Ø 135.00 mm (K) Ø 6.0000 mm.	34
Figure 13: Disc design 2. 8 sample wells. Dimensions for marked areas above: (A) 33.96 mm (B) 5.00 mm (C) 5.83 mm (D) 9.232 mm (E) 23.08 mm (F) 5.84 mm (G) [width] 4.82 mm [height] 6.18 mm (H) 15.00 mm (I) 15.49 mm (J) 21.84 mm (K) 55.60 mm (L) 4.93 mm (M) Ø 10.00 mm (N) 28.40 mm (O) Ø 30.00 mm. Disc diameter: Ø 300.00 mm. ...	35
Figure 14: Disc design 3. 14 sample wells. (A) 5.90 mm (B) Ø 5.00 mm (C) 40.00 mm (D) [height] 6.20 mm [width] 2.84 mm (E) Ø 15.00 mm (F) 7.35 mm (G) 10.26 mm (H) 56.59 mm (I) Ø 8.00 mm (J) 27.07 mm (K) Ø 30.00 mm. Disc diameter: Ø 300.00 mm	35

Figure 15: Disc design 3B. 10 sample wells. (A) 5.90 mm (B) Ø 5.00 mm (C) 40.00 mm (D) [height] 6.20 mm [width] 2.84 mm (E) Ø 15.00 mm (F) 7.35 mm (G) 10.26 mm (H) 56.59 mm (I) Ø 8.00 mm (J) 27.07 mm (K) Ø 30.00 mm. Disc diameter: Ø 300.00 mm	36
Figure 16: Disc design 4. 10 sample wells. (A) Ø 18.00 mm (B) Ø 8.00 mm (C) [height] 5.92 mm [width] 3.63 mm (D) [height] 3.63 mm [width] 6.99 mm (E) [height] 4.67 mm [width] 2.84 (F) Ø 15.00 mm (G) 7.35 mm (H) 10.26 mm (I) 45.04 mm (J) Ø 8.00 mm (K) 34.19 mm (L) Ø 30.00 mm. Disc diameter: Ø 260.00 mm.....	37
Figure 17: Disc design 5. 10 sample wells. (A) 6.60 mm (B) 11.80 mm (C) 9.30 mm (D) 8.38 mm (E) [height] 2.06 mm [width] 2.40 mm (F) [height] 2.06 mm [width] 2.40 mm (G) Ø 1.30 mm (H) 2.17 mm (I) 1.99 mm (J) Ø 10.00 mm (K) 18.11 mm (L) Ø 1.30 mm (M) 14.86 mm (N) Ø 15.40 mm. Disc diameter: Ø 120.00 mm.	38
Figure 18: Disc design 6 (final). 10 sample wells; sample size 300 µL. (A) 6.60 mm (B) 11.80 mm (C) 9.30 mm (D) 8.38 mm (E) 10.98 mm (F) 1.67 mm (G) 11.50 mm (H) Ø 1.30 mm (I) 2.17 mm (J) 1.99 mm (K) Ø 10.00 mm (L) 18.11 mm (M) Ø 1.30 mm (N) 10.20 mm (O) Ø 17 mm. Disc diameter: Ø 120.00 mm.	39
Figure 19: Overhead of microfluidic disc with 10 channels, sample size 300 µL. (11) the well where the reagents for the molybdenum blue method are dried and stored. Samples are added to the disc through the sample inlets at the top. (12) The microchannel where the reacted sample flows from the reaction well into the analysis well. (13) The well where the reacted sample is aligned with the detector and analysed. The shape circled in red is a reference marker used to alignment in disc assembly.....	40
Figure 20: (A) Overview of the finished 2 nd generation system, PhosphaSense_MicroS_D2. Dimensions: 35 cm wide X 30 cm long X 15 cm high; weight: 3 kg; Case: PELI 1400 Case by PELI Products, S.L.U. (B) 880 nm LED and C12880MA micro-spectrometer.	44
Figure 21: Layout of main body of the PhosphaSense_MicroS_D2 system. (A) Spindle/Disc mount, (B) 880 nm LED, LED stand, and micro-spectrometer, (C) LED Display, (D) Power switch, (E) Keypad.....	45
Figure 22: Layout of the inner components of the PhosphaSense_MicroS_D2 system. (A) SD card, (B) LED gamma/intensity adjustment, (C) Battery plug in/port, (D) Battery.	46
Figure 23: Field sample preparation steps for microfluidic analysis. (1) Collect the sample from the source. (2) Filter the sample using a 0.45 µm filter. (3) collect and stored in a sample container before deploying onto the microfluidic disc. Store excess sample according to standardized guidelines ²⁹	47
Figure 24: Illustration of molybdenum blue reaction in the presence of water sample with ortho-phosphate ions as analytes. This reaction forms a coloured molybdenum blue complex.....	54
Figure 25: A single microfluidic disc with a concentration range of 0 - 50 µg P/L. Well 0 is 0 µg P/L, and well 1 is 50 µg P/L. The darker the colour of the reaction, the higher the P concentration.	54
Figure 26: Distribution of combined reagent components within disc well.....	56

Figure 27: Calibration range comparing PhosphaSense_MiniS_D1 to a benchtop spectrometer. Calibration range: 0 – 5 mg/L; wavelength = 880 nm (A) n = 3, %RSD range 0.1 – 7. Equation of the Line: $y = 0.1574x + 0.0225$; $R^2 = 0.9989$. (B) n = 1; Equation of the Line: $y = 0.0338x + 0.003$; $R^2 = 0.9826$ 57

Figure 28: (A) The calibration curve for the laboratory spectrometer (UV-Vis mini – 1240 Shimadzu); wavelength of 880 nm; calibration range of 0 $\mu\text{g PO}_4/\text{L}$ to 500 $\mu\text{g P/L}$; n = 3; Average %RSD 0.4. Equation of the line: $y = 0.0012x + 0.0267$; $R^2 = 0.9626$. (B) PhosphaSense_MicroS_D1 System; wavelength 880.4 nm; calibration range of 0 $\mu\text{g P/L}$ to 500 $\mu\text{g P/L}$; integration time = 0.0001; $n_{\text{well}} = 3$; number of wells per concentration = 2; Average %RSD 2. Equation of the Line: $y = 0.0004x + 0.0073$; $R^2 = 0.979$ 59

Figure 29: Calibration curve with a range of 0 $\mu\text{g P/L}$ to 500 $\mu\text{g P/L}$ demonstrating the reproducibility of the PhosphaSense_MicroS_D2. LED wavelength = 880 nm; integration time = 0.0001; $n_{\text{well}} = 3$; number of wells per concentration = 1; Average % RSD = 0.7. Disc 1: equation of the line: $y = 0.004x + 0.0078$; $R^2 = 0.9698$. Disc 2: equation of the line: $y = 0.0004x - 0.0017$; $R^2 = 0.9733$. Disc 3: equation of the line: $y = 0.0004x - 0.0055$; $R^2 = 0.9715$ 60

Figure 30: Map of sampling sites along the Maiden River in Tubbercurry, Co. Sligo, Ireland.⁶⁰ 62

Figure 31: Field Site A, Monitoring Station T030300. Location: 54° 03' 15.7" N and 8° 43' 52.9" W 62

Figure 32: Field site B, Monitoring Station T020050. Location: 54° 03' 08.2"N and 8° 44' 52.2"W 63

Figure 33: Field site B, near Monitoring Station T020100. Location: 54° 03' 04.5" N and 8° 45' 35.1" W 64

Figure 34: Layout of main body of the system. (A) Spindle/Disc mount, (B) 880 nm LED, LED stand, and micro-spectrometer, (C) LED Display, (D) Power switch, (E) Keypad. 78

Figure 35: Layout of the inner components of the system. (A) SD card, (B) LED gamma/intensity adjustment, (C) Battery plug in/port, (D) Battery..... 79

Figure 36: Main menu screen allowing access to various customization parameters and the analysis run program. 80

Figure 37: Spin speed menu..... 80

Figure 38: Calibration menu..... 81

Figure 39: Integration time adjustment menu..... 82

Figure 40: LED adjustment component 83

Figure 41: LED adjustment menu..... 83

Figure 42: Aligning the disc with the spectrometer; * marks the origin point..... 85

Figure 43: Field sample preparation steps for microfluidic analysis. (1) Collect the sample from the source. (2) Filter the sample using a 0.45 μm filter. (3) collect and stored in a sample container before deploying onto the microfluidic disc. Store excess sample according to standardized guidelines²⁹. 85

Figure 44: Testing locations menu	87
Figure 45: LED and spectrometer stage - side view; screws which need loosened to adjust the stage are highlighted.	90
Figure 46: LED and spectrometer stage - bottom view; screws which need loosened to adjust the stage are highlighted.	90
Figure 47: Control board of system - screws required to loosen for charging the battery are highlighted	91

II List of Tables

Table 1: Definitions on the forms of phosphorus and phosphate found in the environment ^{10,18,19}	5
Table 2: Maximum P Concentrations for freshwater lakes and rivers as set by various governmental agencies/governing bodies.....	9
Table 3: Known interferants for molybdenum blue method, the effects caused by the interferent, and the concentrations required to cause interference. ²⁹	12
Table 4: Summary of P analytical techniques along with their advantages and disadvantages	16
Table 5: The ideal characteristics and a side-by-side comparison of the Phosphaload sensing system vs. PhosphaSense Complete analytical system	25
Table 6: Disc design and optimization summary	41
Table 7: LOD and LOQ of PhosphaSense_MicroS_D2 systems	61
Table 8: Summarization of Data for Field Testing of Phosphasense in Tubbercurry, Ireland.	66

III Abbreviations

AMT: ammonium molybdate tetrahydrate

ABS: acrylonitrile butadiene styrene

DI: Distilled water (18 Ω)

DOC: Dissolved organic Carbon

DO: Dissolved Oxygen

EPA: Environmental Protection Agency

I-EPA: Irish Environmental Protection Agency

K-mono: potassium phosphate monobasic

K-Tart: potassium antimonyl tartrate hydrate

L-AA: L-ascorbic acid

NRF: Nano-Research Facility

P: phosphorus

PMMA: Poly(methyl methacrylate)

PSA: pressure sensitive adhesive

RPS: rotations per second

SHS: sodium bisulfate/sodium hydrogen sulfate

TAP: Total Available Phosphorus

TP: Total Phosphorus

UV-Vis: ultraviolet-visible spectroscopy

WFD: Water Framework Directive

WMS: Water Monitoring Station

IV Acknowledgements

First, I'd like to thank my supervisors, Professor Blánaid White, Professor Fiona Regan, and Professor Nigel Kent, for all of their support, guidance, and understanding throughout my time spent on this project. They have all played a major part in giving me guidance and opportunities throughout my studies at DCU, from lab work to conference presentations.

I'd also like to thank my fellow research group members from the Blánaid White and Fiona Regan research groups for their support, camaraderie, and being a willing ear to discuss issues and ideas with. I would also like to thank Lisa Cronin for all of her help with learning field sampling, as well as being someone I enjoyed travelling to many conferences with and being willing to explore.

I'd also like to thank members of Teagasc, Karen Dally, Sifan Yang, and Linda Heerey, for their help and opinions as members of this project.

Finally, but not least, I'd like to thank my parents, Tim and Julie, sister, Megan, and best friend, Darby, for their unwavering support and encouragement. They have all been my pillars of support, no matter the distance, giving me the fortitude and confidence to follow my dreams when I needed it most.

V Abstract

Development Towards a Complete, Portable Analytical System for the Detection of Phosphate in Freshwater Systems

Rachel Bracker

The eutrophication related to excess phosphorus within our freshwater systems has been a continuous area of concern for environmental scientists and agencies since the implementation of the Water Framework Directive in 2000^{1,2}. While discharge of phosphorus has decreased significantly in Europe over the past twenty-five³ years the issue of phosphorus pollution persists and has started to worsen⁴. Because of trends of increasing phosphorus being reported across Europe, the need for portable, rapid, and reliable phosphate detection is required to determine the sources of excess phosphate and the effects our rapidly changing climate have on phosphorus diffusion.

This research was designed with the goal of developing a low cost, portable, rapid, and complete analytical system for the detection of phosphate in freshwater systems. This new system utilises colorimetric detection of phosphate and the molybdenum blue method dried onto a custom microfluidic disc.⁵ A micro-spectrometer and single wavelength LED enables the system to be compact and easily portable with a comparable performance to its benchtop counterparts. The analytical range of the system is 5-400 µg/L, which encompasses the threshold value of 35 µg/L P for Irish rivers and groundwaters⁶. The system's compact size and weight of less than 2 kg makes it highly portable. With a run time of 15 minutes per ten samples, it enables the *in-situ* detection of phosphate for rapid on-site monitoring. To demonstrate the sensor, three rivers in the northwest of Ireland were identified which have historical orthophosphate readings in the range of 5 - 47 µg/L. With this microfluidic phosphate detection system, rapid *in-situ* detection and reliable, real-time monitoring of phosphorus in freshwater systems was demonstrated.

Chapter 1: Introduction

1.1 Background

In the nearly twenty years since the Water Framework Directive (WFD) was introduced, only 40% of surface waters in Ireland have achieved good ecological status.⁷ Between 1992 and approximately 2015, a decline in the trend of detected phosphorus (P) was detected across monitored countries in the EU. However, since then, there has been a gradual increase in P detected across Europe (Figure 1).

This reversal of the trend in the improvement of detected P has shifted the focus of both research and governmental monitoring efforts from the assessment of ecological status to identifying the appropriate management measures that are needed to achieve good status.⁸ To aid in these efforts, a greater understanding is needed on how P losses from agricultural catchments, deforestation sites, urban areas, and industrial zones will be impacted by our rapidly changing climate.

Numerous efforts have been made to study these trends (discussed further in Section 1.4) via various monitoring and sensing approaches. Despite these advances, there is still a need for a complete, analytical system for the detection of phosphate on-site.⁹

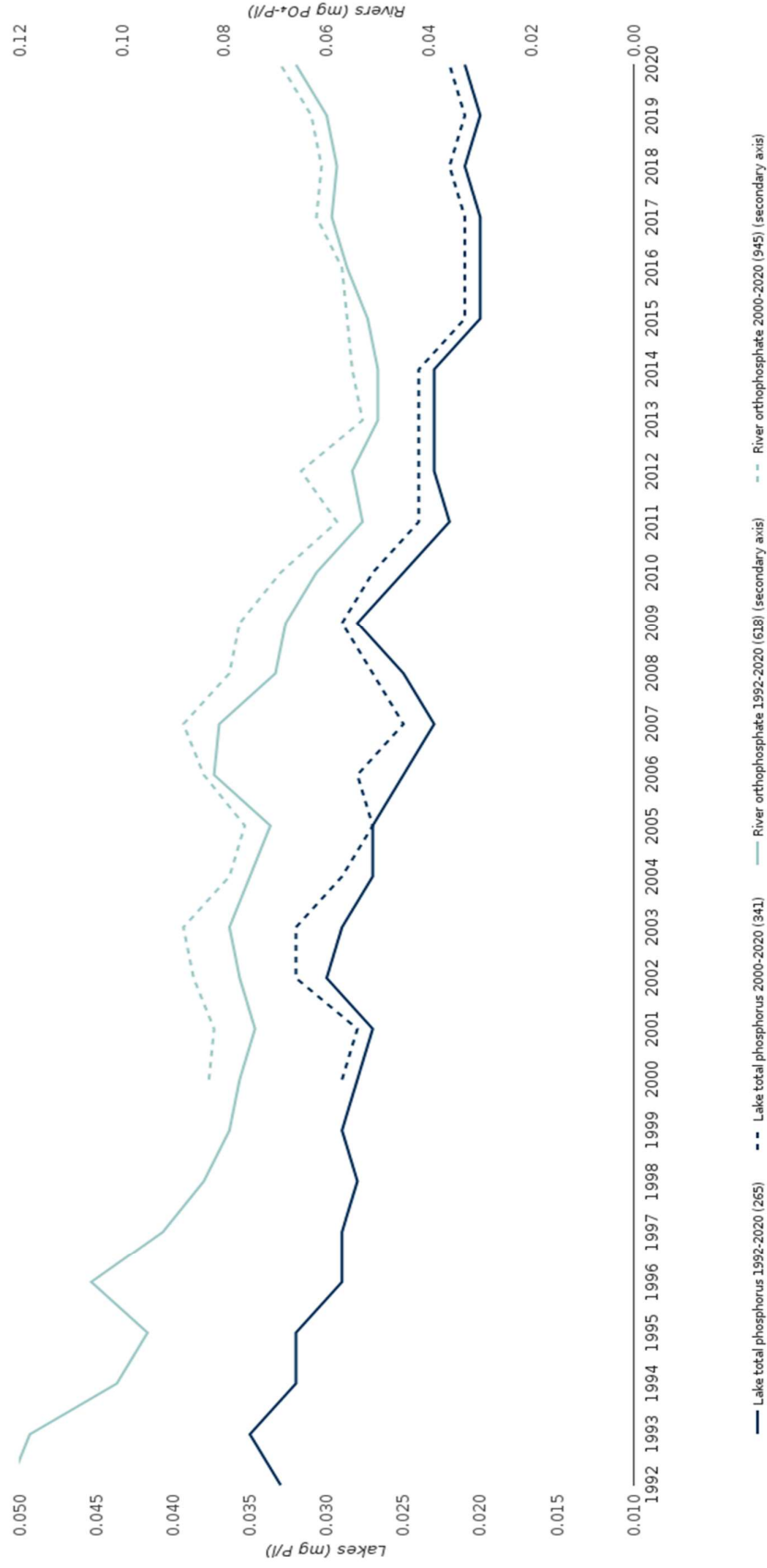


Figure 1: Chart demonstrating the P trends in European lakes and rivers. It shows two time series covering 38 EEA member countries.⁴

1.2 Climate Change and Effects on Phosphorus in the Environment

P is an essential mineral which has a high affinity for soil and sediment particles. Because of this, erosion caused by weather events and human activities allows excess soluble P to rapidly travel through soils and sediments into water systems.¹⁰ While P is essential for life and plant growth, an excess contributes to a process called eutrophication.¹¹ There are several forms of P which can be found in the environment, all of which are discussed in Table 1 below. For the purposes of this study, we are focusing on detecting orthophosphate, which can be found in the total available P (TAP).

As stated by Bergström *et al*, "*Eutrophication of inland and coastal water is one of the largest environmental problems in many countries around the world.*"¹² Eutrophication refers to the hyperfertilisation of water due to nutrients. In fresh water systems, P is considered as the main cause for eutrophication, whereas nitrogen is considered the main cause in coastal waters for this ecological imbalance.^{11,12} This imbalance enables the growth of algae to the point where the algae deoxygenates the water to the detriment of the local flora and fauna of the water system. The most concerning impact of extreme eutrophication is the creation of dead zones, which is defined as areas where the flora and fauna can no longer sustain life.^{11,13} An extreme excess of P is also harmful to humans and other land creatures which use the water source both as a place to drink as well as for recreation.^{13,14} A prevalent example of this is the status of Lake Erie in the United States of America.^{15,16}

One of the biggest pathways for P to travel through is soil and sediments. It is generally considered that most plants only absorb ten to twenty percent of the P applied as fertilizer.¹⁷ The remainder of the P accumulates in the soil and excess, or unabsorbed P

will travel with the soil particulates through erosion and rainfall events into freshwater sources.

Table 1: Definitions on the forms of phosphorus and phosphate found in the environment^{10,18,19}

Phosphorus (P)	<ul style="list-style-type: none"> • An element, found in numerous compound forms or as an ion
Phosphate (PO₄³⁻)	<ul style="list-style-type: none"> • An anion composed of P and oxygen atoms • Can be found naturally as phosphoric salt or phosphoric acid
Total Phosphorus (TP)	<ul style="list-style-type: none"> • The total amount of organic and inorganic P
Organic Phosphorus	<ul style="list-style-type: none"> • A part of living organisms, usually in the form of microbial tissues or plant residue. • Found in the environment most commonly as animal manure and plant debris
Inorganic Phosphorus	<ul style="list-style-type: none"> • Is commonly classified in one of three forms: Plant-available P, adsorbed P, or mineral P
Total available P (TAP)	<ul style="list-style-type: none"> • The fraction of total P that is available for absorption by plants • Can contain orthophosphate and small amounts of organic P • Can be taken up by plants • Can travel easily through the soil via runoff • Also called available inorganic P or soluble P
Unavailable/bound Phosphorus	<ul style="list-style-type: none"> • P that is unavailable for plant uptake • P that is bound in compounds that contain cations such as iron, aluminium, or calcium.

Because P travels so easily through soils and sediments, a major pathway for P to travel from the soil into the water is during erosion and weathering events (Figure 2). Over the past 20 years, the Irish Met Éireann, Irelands National Meteorological Service, have recorded an average increase in the national rainfall at approximately 70 mm (Figure 3).²⁰ Heavy rains and flooding can cause rapid erosion and runoff, causing P from fields and soils to leach into rivers, ponds, and lakes. Because of this, there can be multiple points of entry for P to enter the water systems. This increases the complexity of efforts to monitor the sources of eutrophication, requiring multiple sampling sites and a network of deployment sites.^{13,21}

The Intergovernmental Panel on Climate Change (IPCC) in 2023 has reported unequivocal findings that human influence has caused global warming in the atmosphere which has contributed to extreme weather events including heatwaves, heavy precipitation, tropical cyclones, and droughts all around the world. The report concludes that *“human influence has likely increased the chance of compound extreme events since the 1950s, including increases in frequency of concurrent heatwaves and droughts.”*²² This can cause an increase in the precipitation experienced in Ireland and most northern European countries. Already, as indicated in Figure 3, an increase in rainfall and flooding has been observed in Ireland in recent years. This increases erosion and soil runoff, and in turn increases the movement of phosphate from soil to water¹⁷

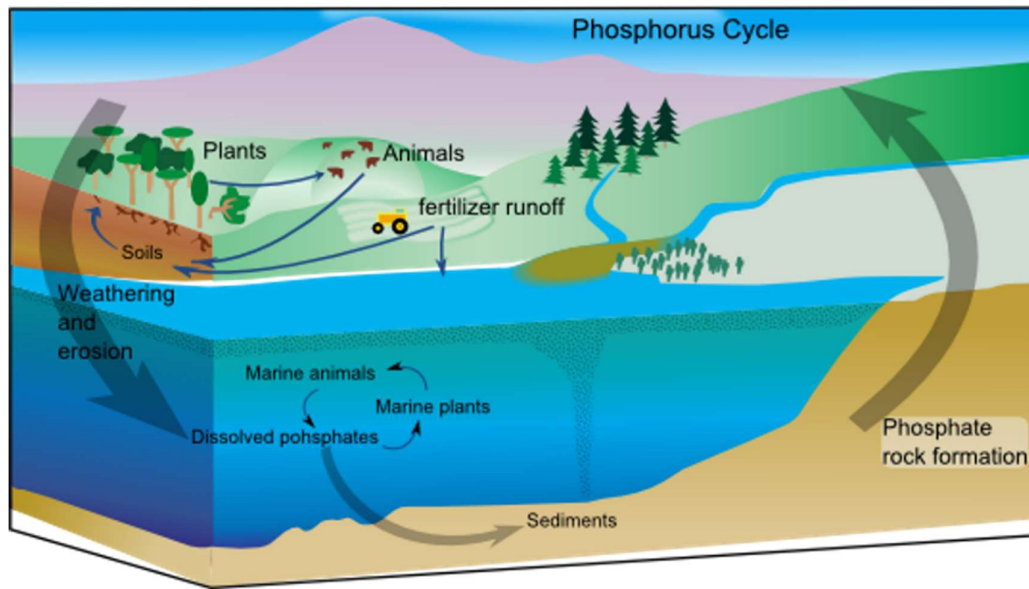


Figure 2: A visual representation of the P cycle as P moves through the environment.¹³

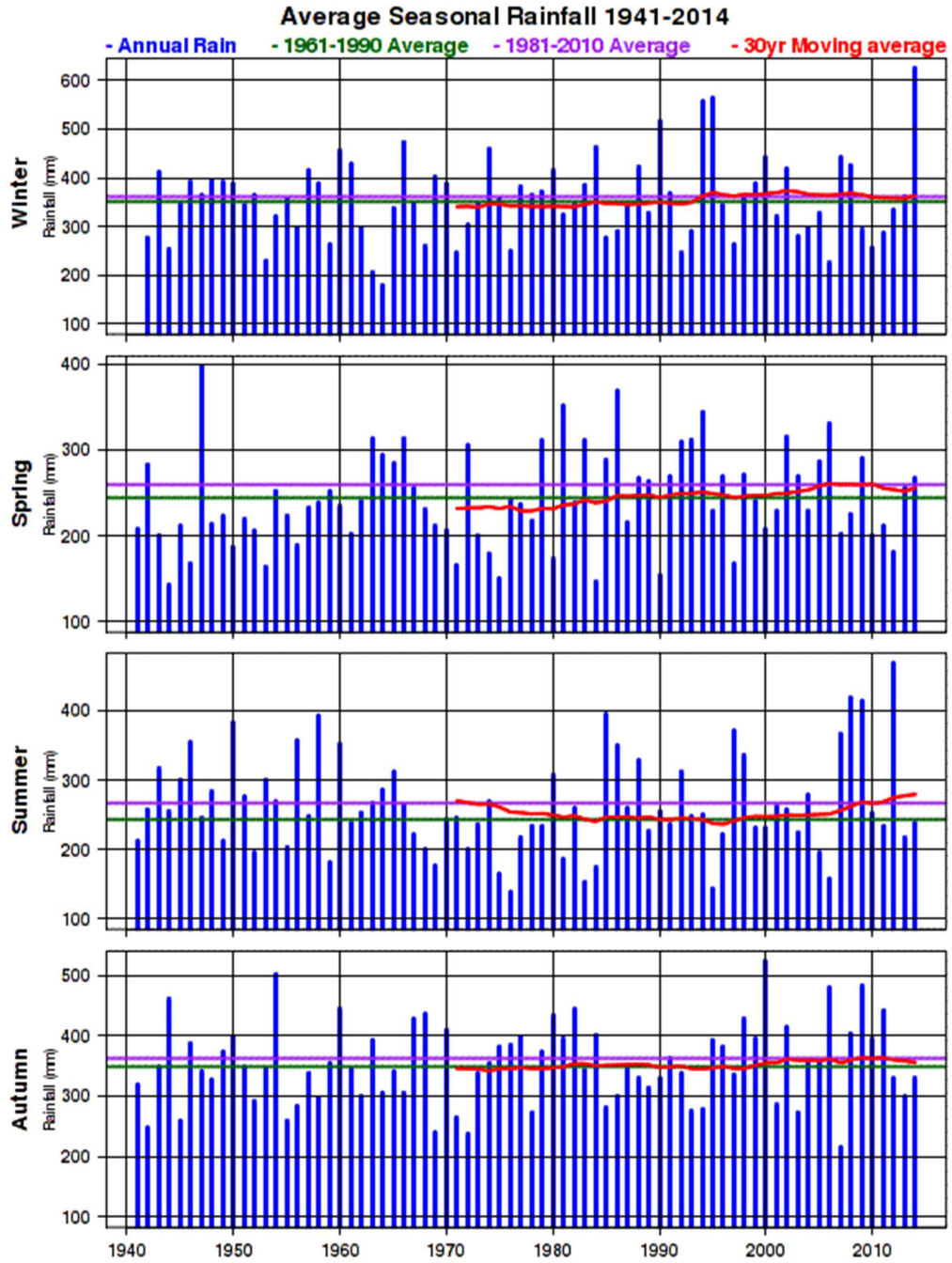


Figure 3: Average Rainfall over 70 years in Ireland²⁰

1.3 Legislation

The Water Framework Directive (WFD) introduced by the European Union requires its members to have a *good* status for all waterbodies, where the water body in question has low levels of influence from human activities and are in a healthy condition^{7,23}. The benchmark for *good* water quality varies between countries and regions, and the criteria relating to P are outlined below in Table 2. For Ireland, the main focus of this thesis, the maximum P concentrations for *good* water quality status outlined by the Irish EPA (I-EPA) is 25 µg P/L for lakes and slow-moving water bodies, and 35 µg P/L for rivers and rapid moving water bodies. Despite these low thresholds, studies have reported that P levels above 20 µg P/L can lead to the overproduction of algae.¹⁴ For those waterbodies which do not have a good status, measures and programmes need to be implemented to minimise phosphorus losses into the water systems.²⁴

Table 2: Maximum P Concentrations for freshwater lakes and rivers as set by various governmental agencies/governing bodies

Country/Governing Body	Maximum P Concentration for Freshwater Lakes for Good Status	Maximum P Concentration for Freshwater Rivers for Good Status
Ireland ²⁵	25 µg P/L	35 µg P/L
United States of America ²⁶	50 µg P/L	100 µg P/L
Europe ²⁷	5 – 500 µg TP/L	8 – 660 µg TP/L
Australia ²⁸	50 µg P/L	100 µg P/L

According to the most recent water quality report released by the I-EPA, only 30% of rivers and 32% of lakes achieved at least the *good* status benchmark. It's been reported that 15% of rivers and 17% of lakes have had an average concentration increase per year since 2016 and 2013 respectively. According to surveys, a high proportion of these findings were in areas with high fertilization rates and poorly draining soils.²⁵ These findings highlight the need for more phosphate monitoring to enable better decision making in regards to P losses into the environment and mitigation measures needed to prevent these losses during extreme weather events.

1.4 Current Methods

There are many traditional methods which can be used in a laboratory to monitor the amount of P in water samples: colorimetric analysis, gravimetric methods, titrations, electrochemical methods, etc.¹⁴ However, even traditional methods have their limitations, such as complex processes, poor stability, or low sensitivity. The most common method used for laboratory analysis is using spectrophotometry and either the Blue or Yellow colorimetric detection method (discussed in Section 1.4.1 below).

With an increase in weather events and the complex nature of many P pathways (discussed in Section 1.2), more frequent water monitoring and an increase in sampling locations along a singular water pathway would be beneficial to a deeper understanding of the effects of weather events. While standard laboratory practices are tried and fairly robust, they are limited in their ability for rapid, repeated analysis in conjunction with grab sampling methods. The main limitation of grab sampling in regards to phosphorus testing is the time required for traveling between the sampling sites and the laboratory, plus the time required for sample preparation before analysis. The lifetime for

phosphorus samples once collected is approximately 48 hours²⁹ and if the samples need to be shipped or the travel is a far distance from the laboratory, then the window for analysis could be short.

To this end, portable analytical devices open the door to more frequent and less limited sampling opportunities than standard in house laboratory procedures.¹³ However, the number of personal trained on the system and available to do the testing does limit the number of samples run and the number of sites which can be visited.

1.4.1. Laboratory Methods

For low levels of P, as low as approximately 10 µg P/L, the molybdenum blue method, also called the Ascorbic Acid Method or the Blue Method, is considered the standard method used to measure P in environmental samples.^{14,31} This method is discussed in more detail in Section 3.3. In most laboratories, the standard liquid version of the method is implemented, however there have been various adaptations of this method developed. Some examples of these adaptations are microfluidic sensors and test strips (shown in Figure 4 below).¹⁴ According to Alam *et al.*, the recognized drawback of this method is that it suffers from poor sensitivity and high levels of interference from species listed in Table 3 below. This method also requires an acidic environment for the most reliable results.^{29,30}

Table 3: Known interferants for molybdenum blue method, the effects caused by the interferent, and the concentrations required to cause interference.²⁹

Interferant	Effect	Conc. Required
Arsenates	Reacts with the molybdate reagent and causes the formation of a blue colour which is similar to the reaction formed with phosphate.	0.1 mg As/L <
Hexavalent Chromium	<ul style="list-style-type: none"> • Produces results which are 3% lower • Produces results which are 10 – 15% lower 	1 mg/L 10 mg/L
NO ₂ ⁻	<ul style="list-style-type: none"> • Produce results which are 3% lower • Produce results which are 10 – 15% lower 	1 mg/L 10 mg/L
Silica ³²	<ul style="list-style-type: none"> • Slower colour change/reaction 	High concentrations of silica in relation to P

Raman spectroscopy is another method which is used to detect the presence of phosphate. Much like the molybdenum blue method, using Raman spectroscopy is highly dependent on pH. However, it is less sensitive UV-Vis due to the weak Raman signal of P and this method is less researched than others for the detection of P.^{14,31,33} Other common laboratory methods include fluorescent or electrochemical detection, which while portable, are not heavily researched, as well as chromatography or mass spectrometry.³⁰ While chromatography and mass spectrometry are accurate methods to calculate the concentration of P in water samples and are well researched, they are not portable and require grab sampling. Table 4 provides a summary of these methods.

1.4.2. New Monitoring Approaches

Alongside standard laboratory techniques, novel phosphate monitoring methods are being developed and perfected, with a major area of focus in portable detection systems. There are a wide variety of portable systems and methods being developed: UV-Vis based systems, including the system developed for this thesis, Raman, and fluorescence based systems and methods.^{5,14,34–36} Examples of these portable systems are shown in Figure 4.

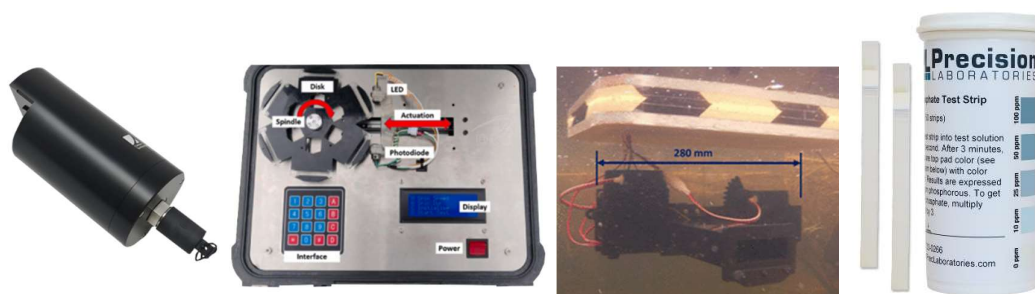


Figure 4: Examples of portable phosphate detection systems. From left to right: UviLux Tryptophan³⁷ fluorescence spectrometer, PhosphaLoad⁵, automatic phosphate sensor developed by Lin *et al.*³⁸, Phosphate Test Strips from Precision Laboratories³⁹

For many of these methods, a microfluidic disc or chip based sensor has been developed.⁴⁰ Of these sensors, colorimetric based sensors utilizing the Molybdenum Yellow Method for P detection, such as the sensor developed by Cleary *et al.*⁴¹, are popular due to their longer shelf life compared to the Molybdenum Blue method²⁹. While the Yellow Method does have a longer shelf life than the Blue Method, it is not as sensitive, having an LOD of 100 $\mu\text{g}/\text{L}$.⁴¹

Grand *et al.* developed a long term P detection system with a much lower LOD of 30 nM. While this system has a good LOD, it would take more units, and therefore more money,

for monitoring multiple locations in a specific time frame than a more portable device.⁴² Another device developed by Lin *et al.* (as shown in Figure 4), was developed for the long term detection of P using the molybdenum blue method and achieved an LOD of 100 µg/L.³⁸

The main benefits of these systems are that they are portable and enable long or short term *in-situ* analysis. However, on average these systems have higher limits of detection than their benchtop counterparts.³⁵ Because of the ability of these systems to be taken to almost any location and the prevalence of eutrophication worldwide, demand for these portable detection methods and systems at affordable prices is increasing. Current research efforts are aiming to bring the standard of these portable systems to a comparable level with their benchtop counterparts.^{14,35,43}

Another method which has emerged within the past two decades is the use of satellite imaging combined with various modelling techniques.⁴⁴⁻⁴⁶ The most common practice for use of satellite imagery for monitoring P is to utilize images taken via electromagnetic waves, visible or infrared light of distant targets and monitor changes found in the images over time. In conjunction with on-site measurements these images can be used to determine changes of P in the water via surrogate measurements as the P present in water bodies does not directly correlate to the optical signals in water. In recent decades, satellite imagery has become a much more affordable and available to researchers.⁴⁴ Because of the satellite being constantly deployed, the ability for frequent sampling is unmatched by most other techniques. However, this benefit is coupled with the drawback that if the satellite does not have a clear line of sight of the sampling location, such as during cloudy days or during a rain event, then data cannot be gathered. Other

factors, such as phytoplankton, turbidity, and total suspended matter can be used to estimate the P concentration.¹⁴

The final method discussed is the use of surrogate sampling. Surrogate sampling is the use of an analyte which mimics the desired analyte, in this case P, within the sample matrix. Recent studies have investigated the use of turbidity and conductivity measurements to estimate the concentration of P.⁴⁷⁻⁴⁹ These measurements are easily taken *in situ*, are quick to measure, and the equipment is highly portable. This enables many measurements to be gathered in quick succession. While these measurements have been found to be good predictors for total P, the error encountered differed widely between sites. It was observed that the correlation between turbidity and total P detected had greater correlation at sites with higher P concentrations.⁴⁷ It has also been observed that a large number of sample readings are needed for reliable datasets, but without autosamplers, the amount of samples needed are often not gathered.⁴⁸ Villa *et al.* recommend further research into the use of modelling alongside surrogate sampling for more accurate P predictions.

Table 4: Summary of P analytical techniques along with their advantages and disadvantages

Source	Method	Advantages	Disadvantages
14	UV-Vis	<ul style="list-style-type: none"> Quantitative and qualitative analysis Well studied, and when combined with the molybdenum blue method, is a standardized analysis method in many countries Relatively low cost 	<ul style="list-style-type: none"> Most methods can be affected by chemical interferants (metals, silica, etc.) Sensitive to external light changes
14,31	Raman	<ul style="list-style-type: none"> Can analyse samples in aqueous and solid forms Rapid analysis Non-destructive methods 	<ul style="list-style-type: none"> Not as researched as other methods for detecting P P has a weak Raman intensity, requiring indirect measurement of P Less sensitive than other methods
14,31	Fluorescence	<ul style="list-style-type: none"> Can analyse a large range of physical parameters, such as fluorescent intensity, quantum yield, fluorescent lifetime, etc. Can be combined with Raman in a technique called <i>in situ</i> hybridization 	<ul style="list-style-type: none"> P has low quantum yield and relatively low energy of a characteristic radiation, hindering detection without indirect methods

14	Satellite	<ul style="list-style-type: none"> • Heavily studied • P concentration is closely related to other water quality parameters such as total suspended matter and turbidity • A cheaper option for long term, routine monitoring of large areas 	<ul style="list-style-type: none"> • Must be combined with on-site measurements for more accurate insight • P does not reflect optical signals in water
47,48	Surrogate Sampling	<ul style="list-style-type: none"> • Common surrogate measurements are turbidity and suspended solids, which can be easily monitored on site 	<ul style="list-style-type: none"> • More research needs done using a surrogate method across multiple, varied sites • Most common surrogate methods are not yet transferrable between sites
50,51	Electrochemical Methods	<ul style="list-style-type: none"> • Can be very selective • Can have very low limits of detection (1.0×10^{-15} M and 7.5×10^{-16} M and 10^{-6} M and 10^{-7} M depending on the electrode used) • Can be analysed at various pH levels • Can preform long-term monitoring 	<ul style="list-style-type: none"> • A newer area of P detection, so not as heavily studied • Stability and reproducibility are generally lower than in other methods

1.5 Conclusions

The need for rapid, portable, monitoring devices for phosphate is a growing area of focus for research and development. Many governments and coalitions are calling for an improvement in water quality and seeking to reduce eutrophication via P to curb algae overproduction. Strides have been made to develop various novel methods to enable more rapid monitoring of P, from models and satellite data to portable sensor systems. This thesis aims to address this much needed area of sensor development and provide a cost-effective, portable, and complete analytical system for phosphate detection in freshwater systems.

1.6 Aims and Objectives

The primary aim is to develop a novel, portable, colorimetric phosphate detection system which meets the needs, in terms of sensing and collection of freshwater phosphate data, discussed in this chapter. Depending on the region and environment in question, there are many different pathways P can travel through. For the purposes of this study, Ireland will be the primary location of interest, but brief consideration will be given to other country's legislation requirements for the purposes of comparison. The Phosphaload_D-PD_2021 that was previously developed in DCU was the start point of this research (Figure 5). Firstly, a new detection system was developed and tested, resulting in the PhosphaSense_MiniS_D1_2021. The second iteration of the detection system, and its incorporation into the portable system, resulted in the development of the PhosphaSense_MicroS_D2_2022-2023 system. This final system also incorporated a new sampling disk.



Figure 5: Timeline of microfluidic system for phosphate development. The iterations of the system developed for this thesis are the PhosphaSense_MicroS_D1 and PhosphaSense_MiniS_D2 (outlined in red).

**Chapter 2: Materials, Methods, and Development of the
PhosphaSense_MiniS_D1 and PhosphaSense_MacroS_D2
Phosphate Detection Systems**

2.1 Introduction, Aims, and Objectives

This chapter provides detail of the development of the PhosphaSense_MicroS_D2 system and the microfluidic discs used. The aim is to develop a portable, complete, analytical system for the on-site detection of phosphate in freshwater systems. This was done by first evaluating the effectiveness of a mini-/micro- spectrometer for the detection of phosphate via the Molybdenum Blue method using the PhosphaSense_MiniS_D1 model. Once the mini-/micro- spectrometer proved sufficient, a micro-spectrometer was then incorporated into the body of the Phosphaload_D-PD-2021 model.

The objectives of this chapter are (1) analyse the benefits and drawbacks of the Phosphaload_D-PD_2021 system designed by Joyce O'Grady and how it can be improved, (2) design and produce a new microfluidic disc design for a vertical spectrometer detection system, (3) design and develop a new microfluidic disc for the PhosphaSense_MicroS_D2 system, (4) and develop a basic operating procedure for the use of the PhosphaSense_MicroS_D2 system.

2.2 Reagents

The chemicals and reagents used were purchased from Sigma-Aldrich Chemical Co., Wicklow, Ireland: sodium bisulphate – technical grade (3.75 M), potassium antimonyl tartrate hydrate – $\geq 99\%$ (0.004 M), ammonium molybdate tetrahydrate – 81.0 – 83.0% (0.32 M), L-ascorbic acid - $\geq 99\%$ (0.1 M), and potassium phosphate monobasic – 99.5-100% (500 $\mu\text{g/L}$). Distilled water (DI) of 18 M Ω was obtained from DCU chemistry was used to create all solutions and dilutions.

2.3 Materials

The plastics used to create the discs were: 3 mm thick X 500 mm X 400 mm Poly (methyl methacrylate) (PMMA) from Access Plastics, 0.5 mm thick X 400 mm X 400 mm PMMA acrylic sheets by Radionics, and 10 m roll of 152.4 mm x 9 mm clear, thick pressure sensitive adhesive (PSA) from Adhesive Research were purchased via the Nano Research Facility (NRF) warehouse at DCU in Dublin, Ireland. 0.45 μ m, 25 mm sterile syringe filters (Sparks Lab) and 15 mL centrifuge tubes (Sarstedt) were also purchased from the NRF warehouse.

All micropipette tips were purchased from Merck, Cork, Ireland. 20 mL disposable syringes and clear 20 mL Wheaton sample vials (DWK Lifesciences) were purchased from Fisher Scientific Ireland Ltd, Spencer Dock, Dublin.

A Bonsenkitchen VS2100 vacuum sealer and Bonsenkitchen vacuum sealer bags (VB3813) were purchased from BonsenKitchen via Amazon.co.uk.

Additional equipment needed for the operation of the microspectrometer developed in this research are a 3 mm hexwrench (for screws attaching the inner components to the metal frame), 2.5 mm hexwrench (for screws securing the disc to the spindle), 1.8 m/m flathead screwdriver (for adjusting the LED intensity), #1 cross-head/Phillips screwdriver (for securing the top of the inner components box to the base of the electrical components box), IPC 30 Lithium Battery Charger [model: 00795-31-3; PRI: 100-240V AC – 50/60Hz 700 mA; SEC: 11.1V $\overline{\text{-----}}$ DC 2000 mA]

2.4 Instrumentation

The benchtop spectrometer used for all experiments was the UV-Vis mini – 1240 Shimadzu spectrometer (Shimadzu Corp, Japan). There were two micro/mini – spectrometers used for the portable systems: a C143834MA-01 Mini spectrometer for the preliminary system, PhosphaSense_MiniS_D1 (Figure 7), and a C12880MA micro-spectrometer (Figure 20) for the PhosphaSense_MicroS_D2 system. For a full operating procedure for the PhosphaSense_MicroS_D2 system, refer to Appendix 2.

PMMA layers were cut using the Epilog Zing16 laser cutter (Epilog, Golden, Colorado, United States), and the PSA layers were cut using the Graphtec CE6000-40 plotter-cutter (Armstrong Ave., Irvine, CA, United States).

2.5 Software

All layers of the microfluidic discs were designed using SolidWorks (<https://www.solidworks.com/product/students>) and AutoCAD software (<https://www.autodesk.eu/products/autocad/overview>).

2.5 Phosphaload diode system and its capabilities/limitations

The Phosphaload system⁴³ (Phosphaload_D-PD_2021 in Figure 6A) was composed of a horizontal 880 nm LED coupled with a photodiode mounted on an actuator (Figure 6B). Disc channel positions for analysis could be selected before starting the run, as well as the spin speed, spin duration, and integration time. Once the desired programming was selected, the disc would spin according to the pre-determined programming and use centrifugal forces to move the liquid sample from the innermost well into the outermost

well. While this system achieved good reproducibility and accuracy, due to the laser cutter creating random imperfections along the sides of the disc during manufacturing along the light path, the system needed recalibrated for each disc.

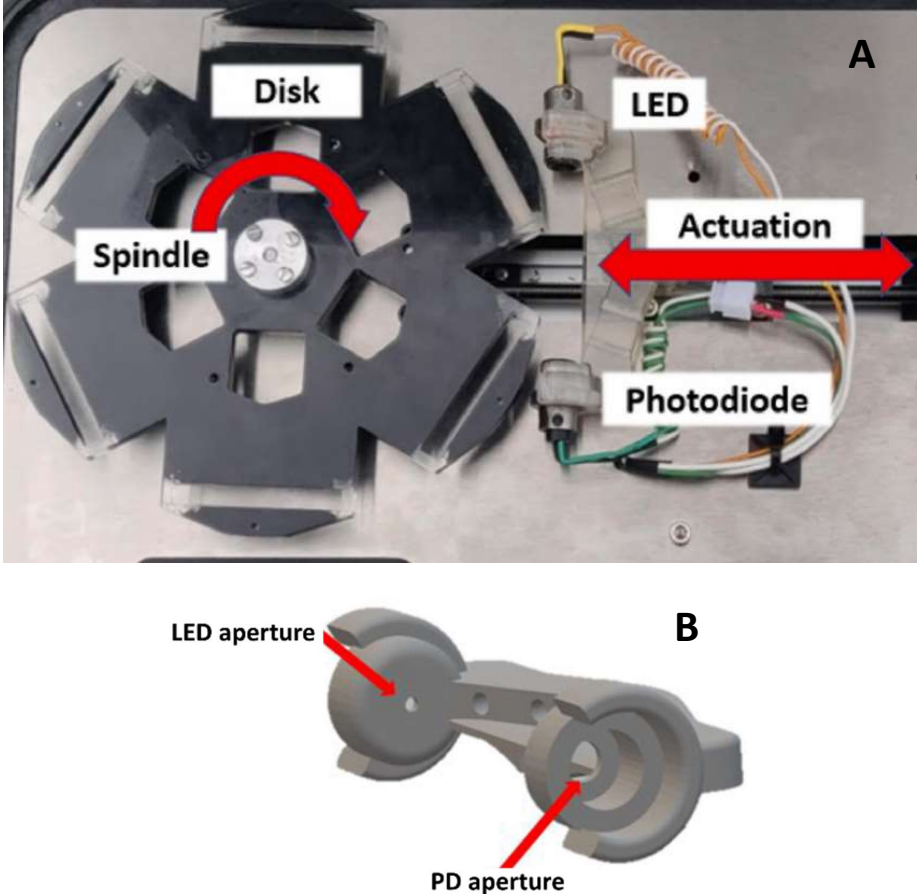




Figure 6: (A) Phosphaload_D-PD-2021 disc, actuator, and LED-Photodiode detector. (B) 1st generation diode/photodiode head. Equipped with OSRAM Opto Semi-conductor LED and 880 nm Silicon Photosensor Photodiode⁴³.

Table 5: The ideal characteristics and a side-by-side comparison of the Phosphaload sensing system vs. PhosphaSense Complete analytical system

Ideal Characteristics	PhosphaSense_MicroS_D2 (PhosphaSense Complete)	Phosphaload_D-PD_2021 (Phosphaload)⁴³
Lightweight	3 Kg	~3 Kg
Compact	35 cm wide X 30 cm long X 15 cm high	35 cm wide X 30 cm long X 15 cm high
Precision/ Reproducible results	%RSD: 1 – 11 LOD: 5 µg/L	%RSD: 7 - 18 ⁴³ LOD: 1.3 µg/L
Easy to use		
Affordable*	€1,320.41	€1,002.20 ⁴³
Number of sample channels (total)	10	6
Number of site samples if two standards and a blank are used	7	3

*Costs for components were bought in small quantities, and manufacturing time and labour is not included. Given this, the costs shown are not a direct comparison with commercial systems on the market but the cost spent for a single unit during this project.

2.6 Optical system redesign Part 1: PhosphaSense_MiniS_D1

The first micro-spectrometer (PhosphaSense_MiniS_D1) used was a Hamamatsu C143834MA-01 Mini-spectrometer, shown in Figure 7. It connected to the computer via a Teensy control board and was housed in an ABS casing which was printed using a 3D printer by the Engineering Department at DCU. The PhosphaSense_MiniS_D1 system was a part of an undergraduate final year project by Harry Beggy where his goal was to update and improve upon the Phosphaload_D-DP_2021 system.⁵⁵ Beggy's goals, as well as the goals for this thesis, were to improve and expand upon the Phosphaload_D-PD_2021 system via the following:

- 1) Remove the need for calibrating the system for every disc;
- 2) Simplify system operation;
- 3) Allow for more samples to be analysed per run;
- 4) Improve upon the LOD/LOQ.

The use of a mini-/micro- spectrometer was determined by Beggy and the engineering team to be the best means of achieving these goals as it removed the main limiting component of analysing across the sides of the disk. Instead, a mini-/mico- spectrometer would allow for a vertical analysis from the top to the bottom of the disk. As is shown in Section 2.7, this singular design change allowed for more space on the disk because:

- 1) The path length of the disk designed by O'Grady was controlled by the width of the channel. For a micro-spectrometer-based system, the pathlength is controlled by the thickness of the disc.*
- 2) The removal of analysing across the sides of the disc removes the need to calibrate the system per disc due to the random imperfections caused in the manufacturing process.

*Because the PhosphaSense_MiniS_D1 did not use a disc for analysis, instead using a raised circular disc designed by Beggy, the path length of this system was controlled by using a spacer (as shown in Figure 7).

After the PhosphaSense_MiniS_D1 proved successful in detecting phosphate via the Molybdenum Blue method (discussed more in Section 3.4.1), the detection system was then adapted for use in the PhosphaSense_MicroS_D2 system. The accuracy and reproducibility of this system were evaluated by me and the mini-spectrometer system

proved to be comparable to a benchtop spectrometer system, as discussed in greater detail in Section 3.4.1.

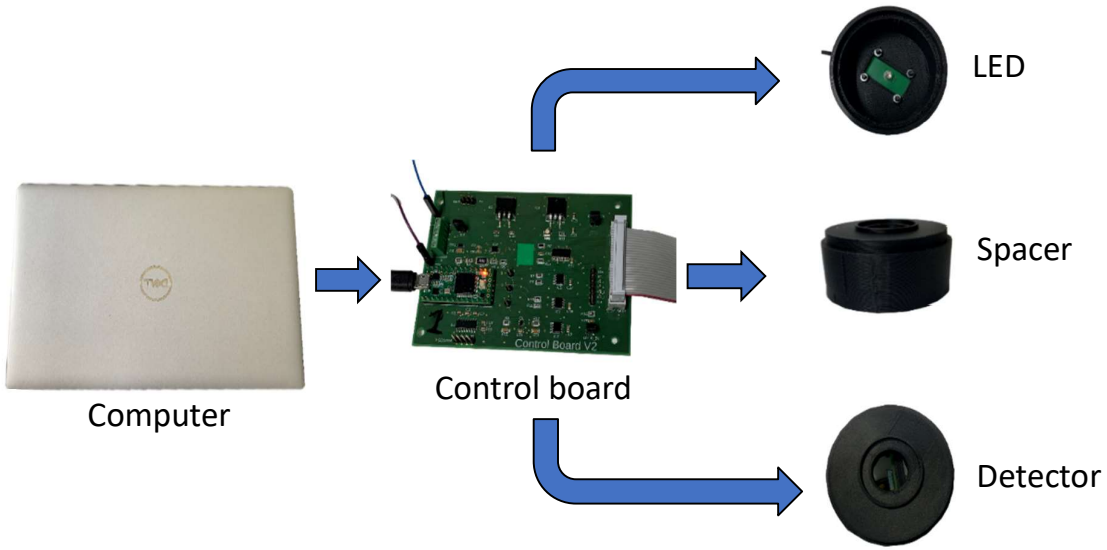


Figure 7: PhosphaSense_MiniS_D1 – Dimensions: 12.5 cm tall X 7 cm diameter. Components: 880 nm IR-LED, Teensy Control Board, and a C143834MA-01 Mini-spectrometer. Casing was 3D printed using ABS.

2.7 Disc optimization

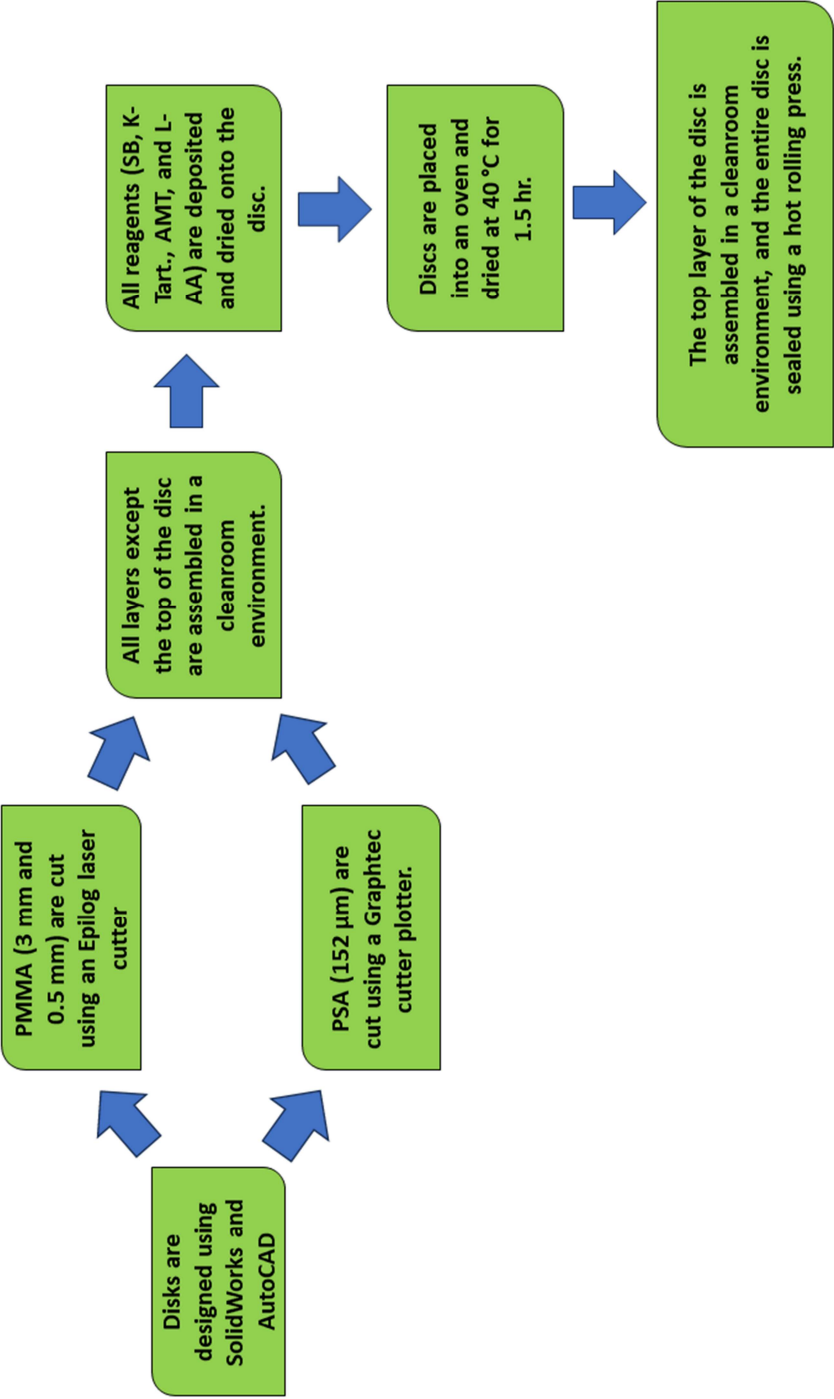


Figure 8: Flow chart outlining the steps of the microfluidic disc manufacturing process from design to final assembly.

2.7.1 – Disc Design Process

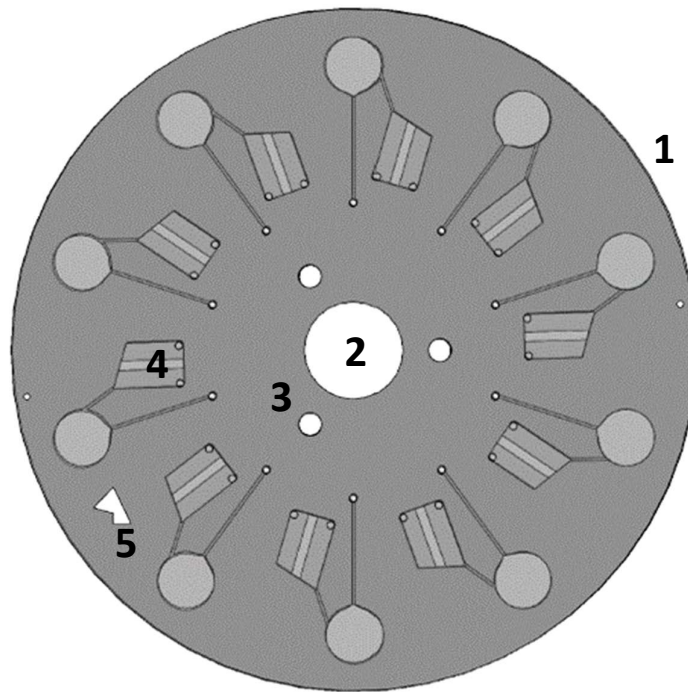


Figure 9: Sections of the microfluidic disc design (1) disc base, (2) spindle mounting point, (3) holes for securing disc to the spindle, (4) microfluidic channel, (5) assembly marker.

All discs were first designed using SolidWorks. All components were created using pre-scribed shapes available within the software that were manipulated using the sizing, trimming, and rotation tools. The base of the disc (Figure 10-1) was created first to provide reference for the spacing available on the disc. For similar reasons, the point in the centre of the disc where the spindle of the system was connected to the disc (Figures 10-2 and 10-3) were drawn onto the disc base with the *Extruded Cut* tool. Next, the microchannel (Figure 10-4) for the second layer was designed. Once designed, the *Circular Sketch Pattern* tool was used to repeat this design around the centre of the disc at even intervals. The *Extruded Cut* tool was used to cut the channel shapes into the disc base. Finally, an assembly marker (Figure 10-5) was created using preexisting shapes and

cut into the disc base using the *Extruded Cut* tool. For a closer look at the dimensions and shapes used for each design, refer to Figures 12 – 19.

This Solidworks file was then saved in .DWG (native file format for AutoCAD⁵²) and .DWF (design web format, makes the file accessible without any specialist software⁵³) formats. This file was then copied, renamed and used as the template for every other layer of the disc. The files for layers 2 and 4 were then imported into AutoCAD and exported as .DXF files. Finally, the files were downloaded onto the computer in the fabrication lab and the PSA layer files were converted into .GSD format (General Station Description file, a device specific file format⁵⁴) prior to printing.

PMMA layers were cut using the Epilog Zing16 laser cutter, and the PSA layers were cut using the Graphtec CE6000-40 plotter-cutter following the procedure provided by the DCU NRF fabrication laboratory technician.

Discs were then assembled by hand in a clean room, using the mountain shaped marker on the outside of the disc (circled in red in Figure 19) to properly align the wells. After all but the top layer was assembled, discs were compressed using a hot roll laminator to activate the PSA.

Next, the discs were taken to the chemical laboratory and the combined reagent was applied to the disc (Section 2.10.1). After the reagents were dried and the disc cooled, the top layer was attached to the disc. Finally, the discs were sealed in bags using a vacuum sealer and stored at room temperature in a dark location. Current shelf life of the discs is one week.

2.7.2 – Layers of a Disc

The top layer of the disc was made of 0.5 mm PMMA and consisted of two sample inlet points and one air vent for each channel. This is shown as Layer 1 in Figure 10. The second layer was composed of PSA and served two main purposes: the first was to seal the top and middle PMMA layers, and the second was that this layer composed the microchannels which allowed the sample to flow between each well.

Layer 3 was composed of 3 mm PMMA and served as the main component for the pathlength of the microfluidic disc. The third layer did not have any microfluidic channels and only had the shape of the wells where sample/liquid would rest and an air vent. The fourth layer mirrored the third, composed of PSA to adhere the middle and bottom layers of the disc, with one exception: two tabs of PSA which extended into the innermost well for the combined reagent to dry onto. Finally, the fifth layer, composed of 0.5 mm PMMA, served to seal the bottom of the disc and had no unique cutouts beyond the holes for mounting the disc to the spindle.

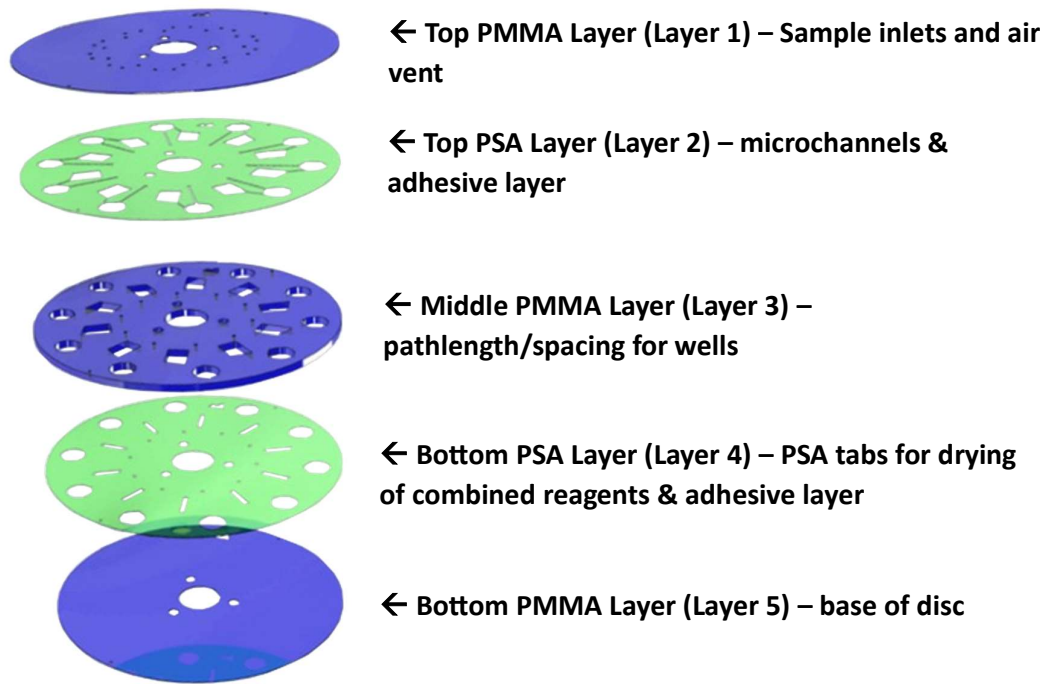


Figure 10: Blue layers are PMMA plastic, the top and bottom layers are 0.5 mm and the middle layer is 3 mm PMMA. The green layers are pressure sensitive adhesive (PSA) used to create the microchannels and bind each layer together.

2.7.3 – Disc Design Iterations

Figures 12 – 19 show each iteration of disc designs through the lifetime of the project. Details of the reasoning behind the changes as well as the advantages and disadvantages of these changes are discussed in detail below and in Table 6.

To save on materials and time, discussions and theoretical troubleshooting based on past experiences of the team took place before any design (Figures 18 and 19) were manufactured. This was in part due to my designing of the discs from a chemist’s perspective and wanting to verify the validity of my designs with those with engineering expertise and more experience with microfluidic discs before manufacturing.

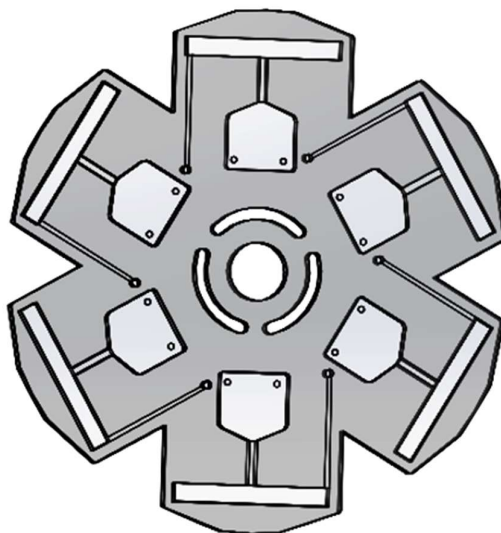


Figure 11: Microfluidic disc design by Joyce O’Grady for Phosphaload_D-PD_2021. 6 sample wells; sample volume 600 μ L; detection system: horizontal diode/photodiode.

Figure 11 shows the original disc as designed by Joyce O’Grady. While this disc worked well for the Phosphaload_D-PD_2021, there were a few drawbacks that this project planned to improve upon. The two major modifications which were needed were:

- 1) Remove the need for constant recalibration due to random imperfections brought on during the manufacturing process by designing for a top-down detection method.
- 2) Increase the number of sampling sites on the disc to allow for more efficient analysis.

The original disc of the Phosphaload_D-PD_2021 system designed by Joyce O’Grady⁴³ was created to accommodate the horizontal diode/photodiode (discussed further in Section 2.5.). Therefore, it was restricted to the snowflake disc pattern to enable the diode/photodiode to align itself with the well containing the reacted analyte. The Phosphaload_D-PD_2021 disc had 6 channels for individual analysis which could hold a sample size of 600 μ L.

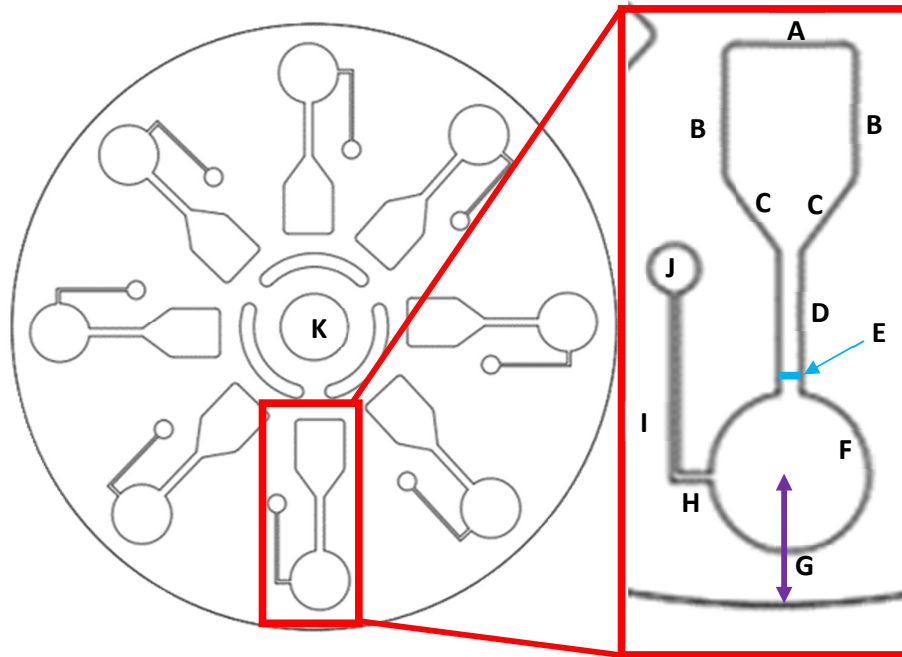


Figure 12: Disc design 1. 8 sample wells with sample volume of 500 μ L. Dimensions for areas marked above: (A) 10.4142 mm (B) 10.6744 mm (C) 6.2795 (D) 11.9174 mm (E) 1.8147 mm (F) \varnothing 13.2310 mm (G) 9.7888 mm (H) 3.3336 mm (I) 15.7945 mm (J) 4.000 mm (Disc diameter) \varnothing 135.00 mm (K) \varnothing 6.0000 mm.

The first design (Figure 12) for the new disc took elements from the original disc (Figure 11) while attempting to reduce the sample size needed to allow for more channels to be incorporated onto the disc. While this preliminary design did allow for more channels to be added, it was decided that there could be a more efficient use of disc space by rearranging how the components of the combined reagent were dried onto the disc. This would enable the inner most well to be smaller in size and potentially allow for more channels to be added. There were also concerns raised by the DCU Engineering group we were working with that the air vent on the left side of the channel was improperly placed and liquid would flow into the vent.

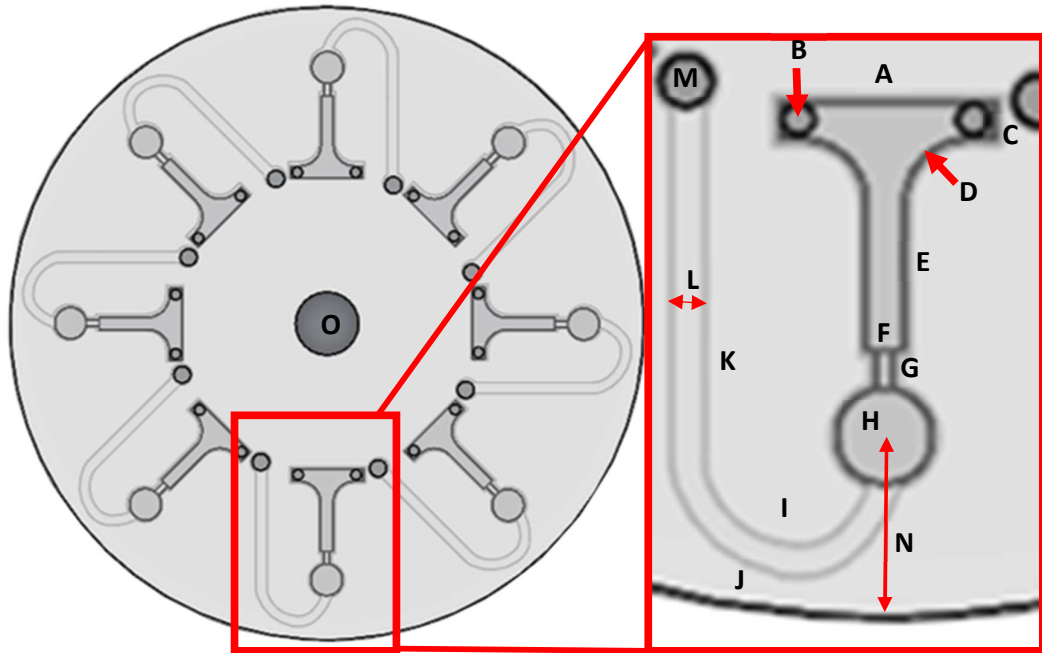


Figure 13: Disc design 2. 8 sample wells. Dimensions for marked areas above: (A) 33.96 mm (B) 5.00 mm (C) 5.83 mm (D) 9.232 mm (E) 23.08 mm (F) 5.84 mm (G) [width] 4.82 mm [height] 6.18 mm (H) 15.00 mm (I) 15.49 mm (J) 21.84 mm (K) 55.60 mm (L) 4.93 mm (M) \varnothing 10.00 mm (N) 28.40 mm (O) \varnothing 30.00 mm. Disc diameter: \varnothing 300.00 mm.

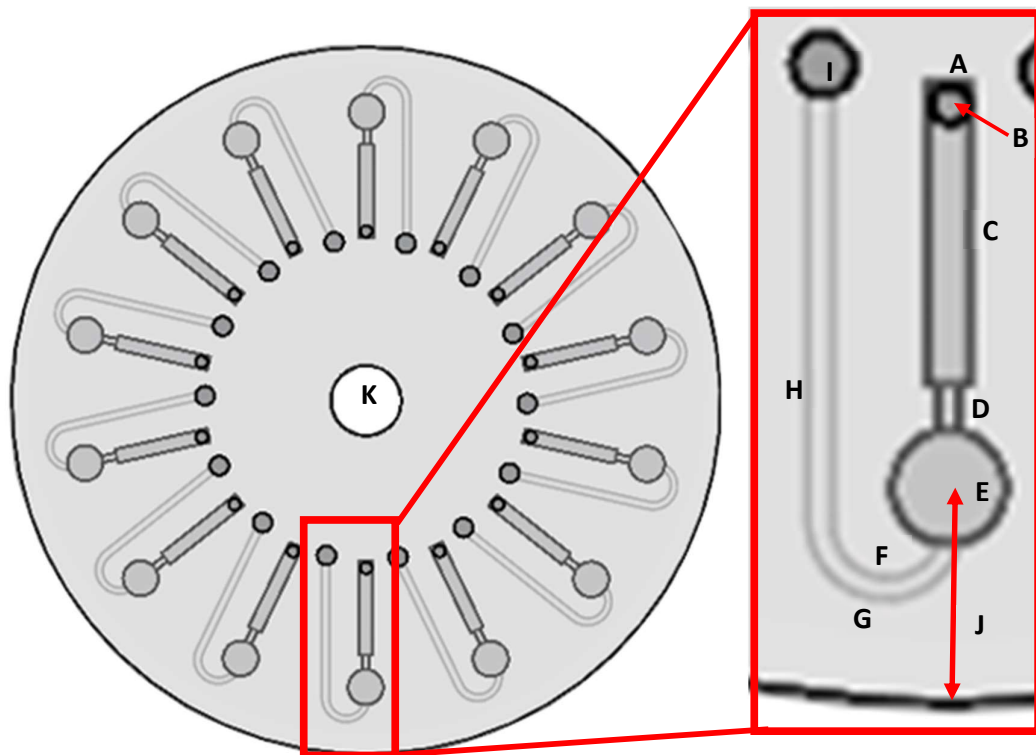


Figure 14: Disc design 3. 14 sample wells. (A) 5.90 mm (B) \varnothing 5.00 mm (C) 40.00 mm (D) [height] 6.20 mm [width] 2.84 mm (E) \varnothing 15.00 mm (F) 7.35 mm (G) 10.26 mm (H) 56.59 mm (I) \varnothing 8.00 mm (J) 27.07 mm (K) \varnothing 30.00 mm. Disc diameter: \varnothing 300.00 mm

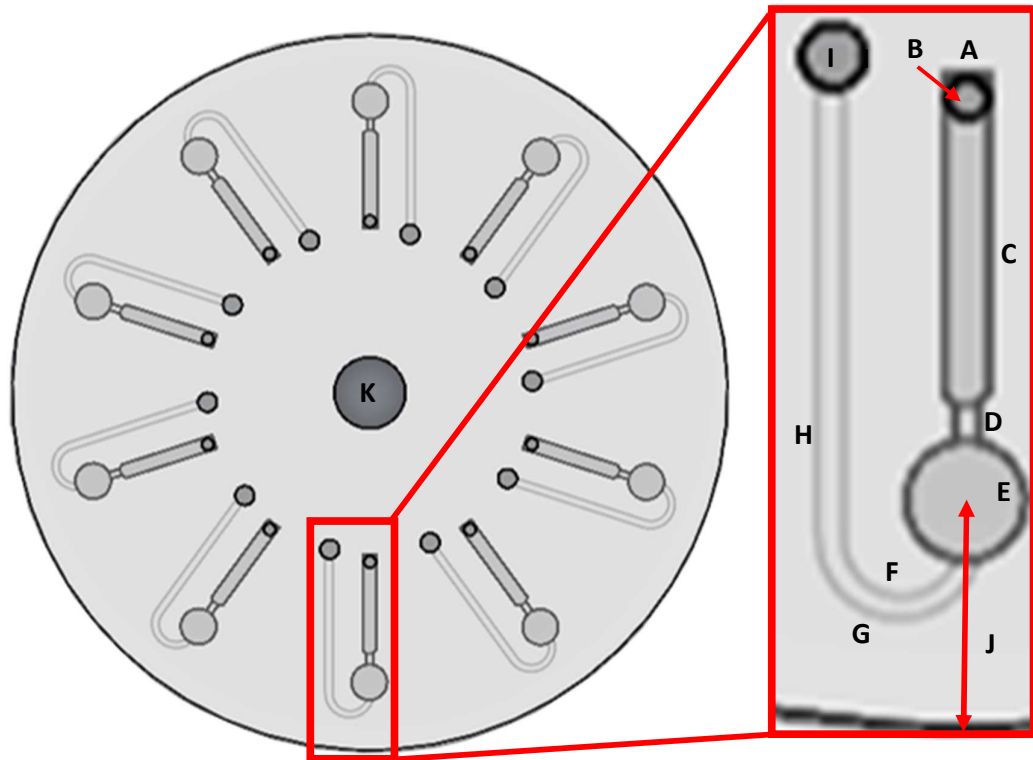


Figure 15: Disc design 3B. 10 sample wells. (A) 5.90 mm (B) \varnothing 5.00 mm (C) 40.00 mm (D) [height] 6.20 mm [width] 2.84 mm (E) \varnothing 15.00 mm (F) 7.35 mm (G) 10.26 mm (H) 56.59 mm (I) \varnothing 8.00 mm (J) 27.07 mm (K) \varnothing 30.00 mm. Disc diameter: \varnothing 300.00 mm

The next design reduced the space needed for the innermost well by narrowing the width of the well. Three designs were created with this concept in mind (Figures 15-17). The first (Figure 15), had two sample inlet points and eight channels in total, still marginally inspired by the original disc (Figure 11). After this design was prototyped in SolidWorks, it was questioned if the two sample inlets were necessary and took up unnecessary space. This led to the design shown in Figure 14, which has one sample inlet and 12 channels. After further discussion with the Engineering team, it was decided that the channels in Figure 14 were too close together and would risk easy breakage during the manufacturing process due to the thinness of the 0.5 mm PMMA. Therefore, the

design in Figure 15 was generated which had ten channels spaced further apart to uphold the integrity of the thin PMMA.

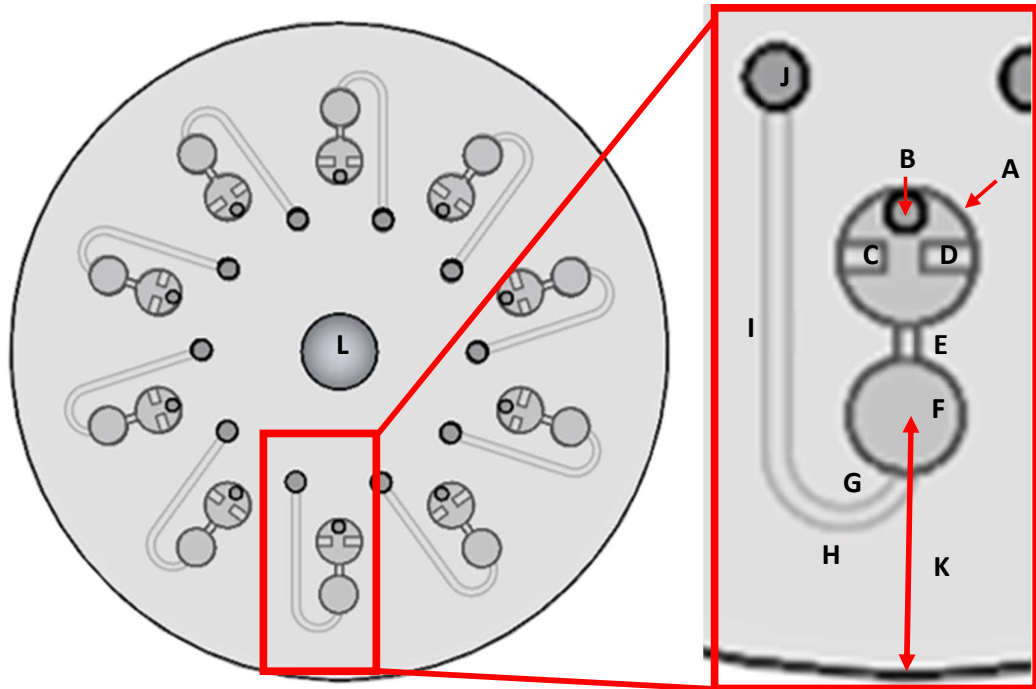


Figure 16: Disc design 4. 10 sample wells. (A) \varnothing 18.00 mm (B) \varnothing 8.00 mm (C) [height] 5.92 mm [width] 3.63 mm (D) [height] 3.63 mm [width] 6.99 mm (E) [height] 4.67 mm [width] 2.84 (F) \varnothing 15.00 mm (G) 7.35 mm (H) 10.26 mm (I) 45.04 mm (J) \varnothing 8.00 mm (K) 34.19 mm (L) \varnothing 30.00 mm. Disc diameter: \varnothing 260.00 mm.

After further consideration and discussion of the design in Figure 15, concerns about the ease of drying the reagents within the innermost well, as well as the ability of the sample to move and mix within the well were raised. This prompted a redesign of the innermost well to match that seen in Figure 16, with a circular shape used for both the inner and outer wells. Strips of PSA were added to the lower most PSA layer as locations for the combined reagents to dry onto in place of cutting out separate circles of PSA, as was used in the original disc design by Joyce O’Grady. The design in Figure 16 kept the number of channels at ten for structural integrity.

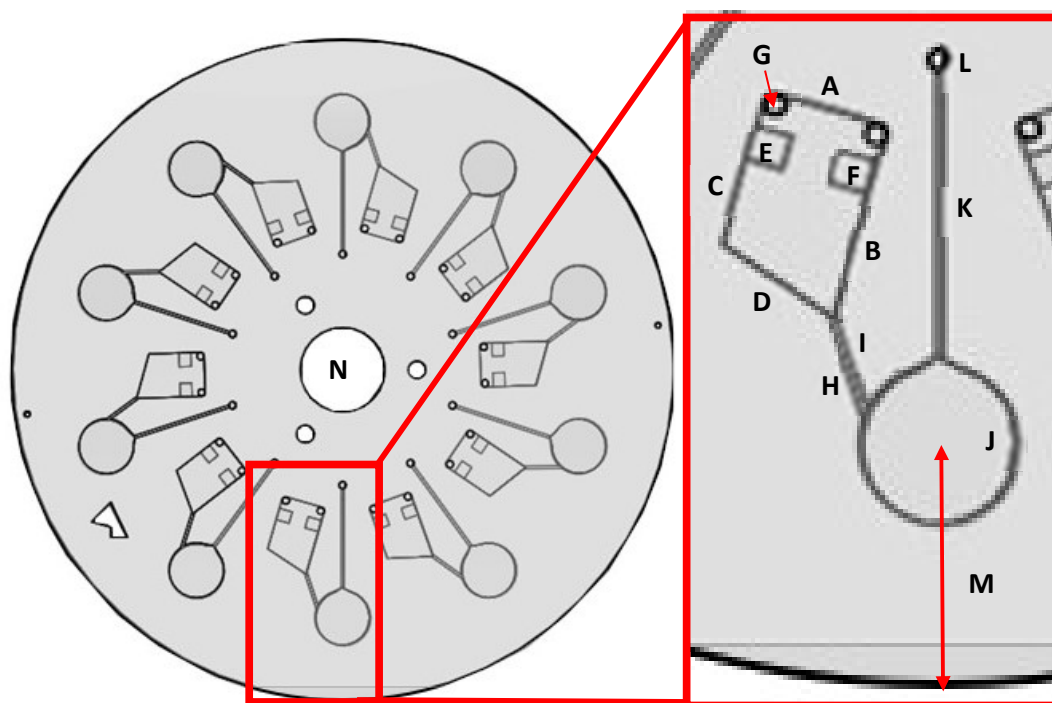


Figure 17: Disc design 5. 10 sample wells. (A) 6.60 mm (B) 11.80 mm (C) 9.30 mm (D) 8.38 mm (E) [height] 2.06 mm [width] 2.40 mm (F) [height] 2.06 mm [width] 2.40 mm (G) \varnothing 1.30 mm (H) 2.17 mm (I) 1.99 mm (J) \varnothing 10.00 mm (K) 18.11 mm (L) \varnothing 1.30 mm (M) 14.86 mm (N) \varnothing 15.40 mm. Disc diameter: \varnothing 120.00 mm.

Further discussion around the design with the entire team raised concerns of the sample flow from the innermost well into the outermost well due to the lack of a funnel shape to help guide the liquid downward. Dr. Dave Kinahan was then consulted due to his main research using and designing microfluidic discs. His suggested design, shown in Figure 17, was altered slightly to incorporate a larger inner well and two square areas for the combined reagents to dry. Three versions of this disc were designed, one with an outer well diameter of 5 cm, a second with an outer well diameter of 10 cm, and a third with an outer well diameter of 15 cm.

Flow tests were then conducted to determine if the discs performed as theoretically expected when spun with liquid, and if so, which of the three designs had the best flow. The design using a 10 cm diameter outer well displayed the most consistent drainage from the inner well into the outer well among the discs tested.

Finally, the discs were tested on the PhosphaSense_MicroS_D2 system itself, and two final adjustments were made to the design. The first adjustment moved the location of the channels outwards and closer to the edge of the disc. This change was made because the LED and micro-spectrometer could not reach the outermost well on the disc shown in Figure 17. The other change was to enlarge the tabs of PSA used to dry the components of the combined reagent to make application of the reagents easier. These changes culminated in the disc shown in Figure 18.

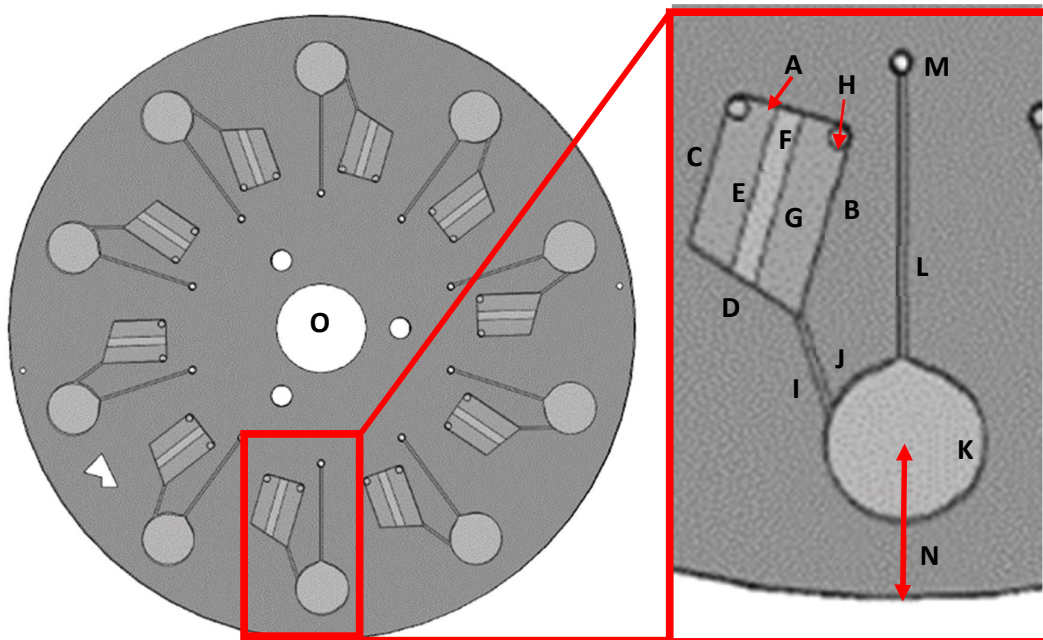


Figure 18: Disc design 6 (final). 10 sample wells; sample size 300 μ L. (A) 6.60 mm (B) 11.80 mm (C) 9.30 mm (D) 8.38 mm (E) 10.98 mm (F) 1.67 mm (G) 11.50 mm (H) \varnothing 1.30 mm (I) 2.17 mm (J) 1.99 mm (K) \varnothing 10.00 mm (L) 18.11 mm (M) \varnothing 1.30 mm (N) 10.20 mm (O) \varnothing 17 mm. Disc diameter: \varnothing 120.00 mm.

The design of the wells on the disc, as shown in Figure 18, allows for the flow of analyte after reaction with the combined reagent from area 1 into area 3 using centrifugal force produced as the disc is spun by the system. Once the sample is in the outer well, it is analysed by the micro-spectrometer (further discussed in Section 2.10.3).

Overall, the final disc design (Figure 19) has the space for 10 samples: a blank or control, two standards for calibration, and seven field samples. This enables the analysis of up to seven replicates per analysis, or one sample for seven individual sampling sites depending on the desired analysis. The sample size required is 300 μL . Due to the microchannels being so thin, all samples need to be filtered to prevent the microchannel from clogging due to small sediment or debris.

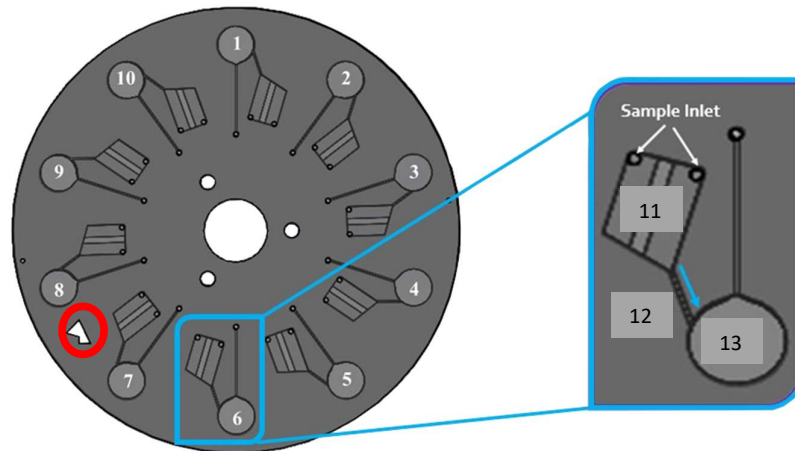


Figure 19: Overhead of microfluidic disc with 10 channels, sample size 300 μL . (11) the well where the reagents for the molybdenum blue method are dried and stored. Samples are added to the disc through the sample inlets at the top. (12) The microchannel where the reacted sample flows from the reaction well into the analysis well. (13) The well where the reacted sample is aligned with the detector and analysed. The shape circled in red is a reference marker used to alignment in disc assembly.

Table 6: Disc design and optimization summary

Figure	Disc Design	Changes Made	Number of Wells	Advantages	What went wrong/disadvantages
11	Original	None	6		Due to analysis being across the length of the disc, and random imperfections created on the sides of the disc during assembly, each disc needed a separate calibration.
12	1	Based largely off of the original design (Figure 2). Changed the long, outermost well into a circular design for the vertical spectrometer.	8	Circular lower well design was better suited for detection using the vertical LED/spectrometer detection system than the original design.	Not a good optimization of disc space. Placement of the air-vent channel could allow liquid to flow out of the outermost well.
13	Design 2	Narrowed the innermost well and shrunk the size of the outermost well.	8	Channels take up less space on the disc.	The square design of the bottom of the innermost well might not allow for liquid to flow to the outermost well.
14	Design 3	Removed one of the sample inlet points	14	Six more channels than in previous iterations of the disc design.	Channels are so close together that it risks cracking the uppermost, thin

				Extremely simple design	layer of the disc during assembly. The square design of the bottom of the innermost well might not allow for liquid to flow to the outermost well.
15	Design 3B	Removed four of the channels. Tapered the bottom of the innermost well to allow for liquid flow.	10	Channels are adequately spaced so as to not threaten the integrity of the thinner PMMA. Space efficient design.	The narrow channel might not allow for adequate sample mixing/flow.
16	Design 4	A circular design was used in place of the rectangular design for the innermost well. Tabs of PSA were included in the design to dry the combined reagents onto to remove the need to cut out separate PSA Tabs.	10	PSA cut-outs for innermost well removed the need to separately cut out PSA circles for the combined reagent. The circular, inner well, design allowed for better sample mixing.	Need to taper the bottom of the circle to allow for better liquid flow into the outermost well.

17	Design 5	An offset, semi-rectangular design replaced the innermost circular well.	10	The new design for the inner well allowed space for adequate sample mixing while allowing for consistent liquid and air flow.	PSA tabs for the combined reagents were too small. Channels were too far in on the disc to reach the detector.
18	Design 6	Channels were moved towards the outer edges of the disc. PSA tabs for the combined reagents were enlarged.	10	There was adequate space for combined reagents to be placed. The outermost well could be reached by the detector.	

2.8 Optical system redesign Part 2: PhosphaSense_MicroS_D2

Upon proving that the PhosphaSense_MiniS_D1 was comparable in quality to a benchtop system, a C12880MA micro-spectrometer was installed into the casing of the Phosphaload_D-DP_2021 system (Figures 6 and 20), replacing the LED/photodiode detector. This became the PhosphaSense_MicroS_D2. Initial testing consisted of calibration line comparisons and the reproducibility of data both within a single disc and across multiple discs. The results of these studies are discussed in detail in Section 3.4.2. This study is preliminary in nature, with the goal to prove that it is capable of analysing freshwater samples for phosphate. Therefore, studies into parameters such as noise, stability/drift, and the effects of temperature were not conducted. These studies should be carried out in future work with the system.

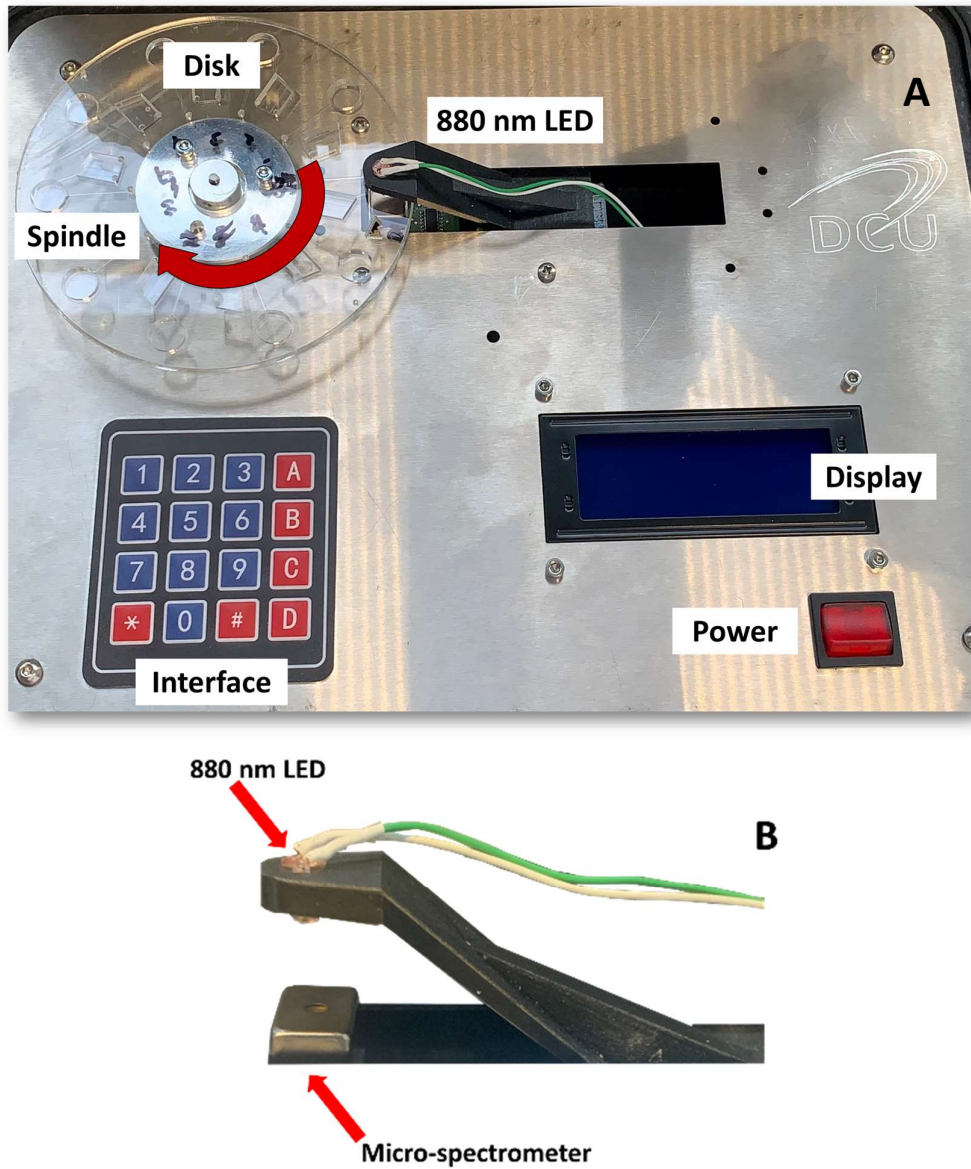


Figure 20: (A) Overview of the finished 2nd generation system, PhosphaSense_MicroS_D2. Dimensions: 35 cm wide X 30 cm long X 15 cm high; weight: 3 kg; Case: PELI 1400 Case by PELI Products, S.L.U. (B) 880 nm LED and C12880MA micro-spectrometer.

2.9 PhosphaSense Complete analytical system – Improvements on the Phosphaload System

In the Phosphasense_MiniS_D1, a new detection system was developed, though was not integrated into the Phosphaload_D-DP_2021 system. Once this new detection

system had been optimised, a micro-spectrometer was integrated into the Phosphaload_D-DP_2021 system, and a new sampling disk was also designed. The resulting final Phosphasense_MicroS_D2 system consists of three main components: the main body of the system itself (shown and detailed in Figure 21), the inner electrical components (shown and detailed in Figure 22), and the microfluidic disc (shown and detailed in Figure 19).

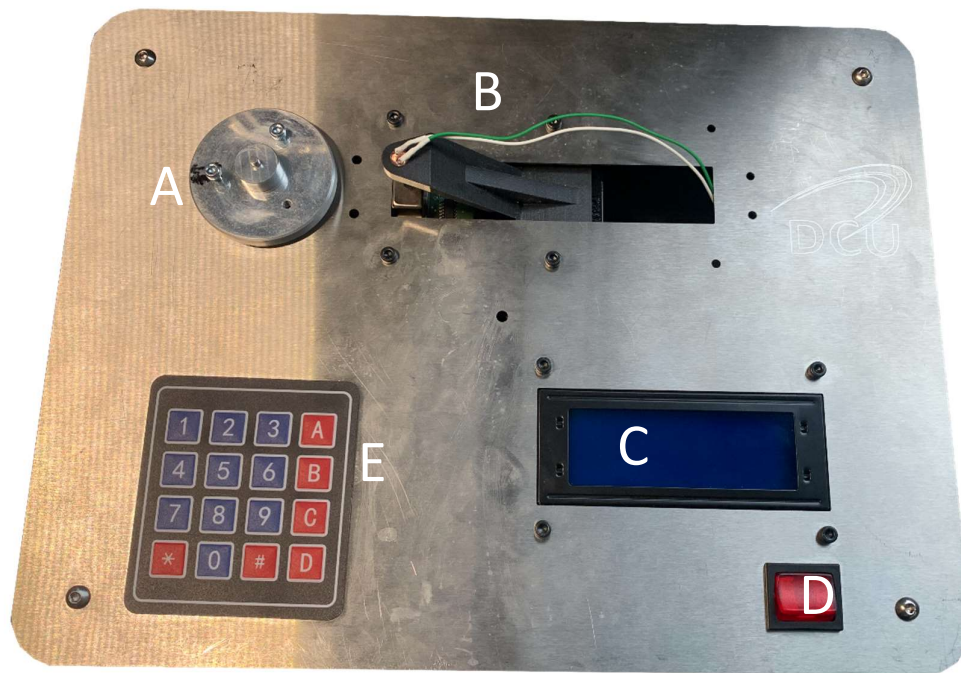


Figure 21: Layout of main body of the Phosphasense_MicroS_D2 system. (A) Spindle/Disc mount, (B) 880 nm LED, LED stand, and micro-spectrometer, (C) LED Display, (D) Power switch, (E) Keypad.

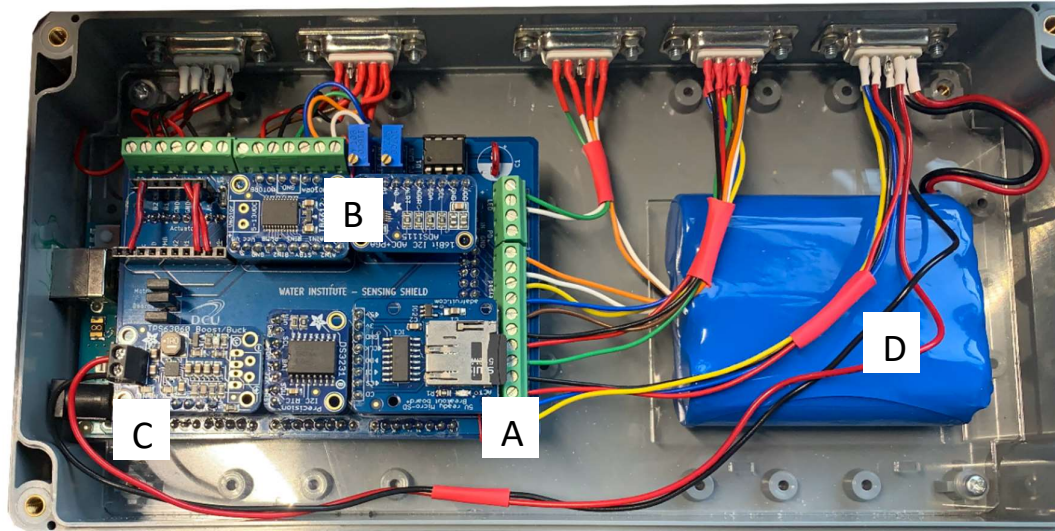


Figure 22: Layout of the inner components of the Phosphasense_MicroS_D2 system. (A) SD card, (B) LED gamma/intensity adjustment, (C) Battery plug in/port, (D) Battery.

2.10 Description of operating procedures for PhosphaSense Complete

2.10.1 Sample Preparation and Deployment on Disc

The preparation required for field samples is to filter the sample through a 0.45 μm filter and then store the sample in a plastic, watertight container. For experiments shown in this document, a 15 mL centrifuge tube was utilized. This process is summarised in Figure 23.

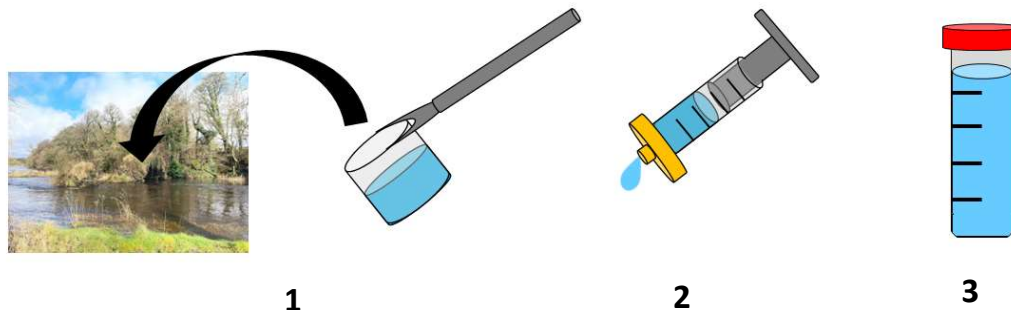


Figure 23: Field sample preparation steps for microfluidic analysis. (1) Collect the sample from the source. (2) Filter the sample using a 0.45 µm filter. (3) collect and stored in a sample container before deploying onto the microfluidic disc. Store excess sample according to standardized guidelines²⁹.

After collection and filtration, samples can be deployed directly onto the disc using a micropipette or syringe. The sample is injected through the sample inlets shown in Figure 19, and 10 minutes are allotted for the sample to react with the combined reagents. Once the reaction is complete, the analysis program is run on the system (discussed in more detail below) and the results are displayed on the LCD screen on the system and stored on the SD card within the system for later analysis. The settings for the samples discussed in this thesis are: spin speed = 60 rps, spin time = 30 seconds, integration time = 0.001 seconds.

Any excess sample which is collected and stored for later analysis must be kept in a cool environment and should be stable for approximately 48 hours²⁹.

2.10.2 – PhosphaSense System Customization Options

For a full, detailed operating procedure of the PhosphaSense_MicroS_D2, refer to Appendix 2.

The PhosphaSense_MicroS_D2 system allows for user customization of most experimental parameters. The parameters which can be adjusted are:

- Disc spin speed
- Disc spin duration
- LED intensity
- Integration time

All parameters except for LED intensity are automatically set to their default settings (as described at the end of Section 2.10.2.) and will need adjusting each time the system is turned on. The LED intensity is adjusted manually on the control board (as described in Appendix 2, Section A2.2) and should be checked at least once a month. Unless the system is jostled regularly, it should not need adjusting more than two or three times a year.

2.10.3 – Analysing a Disc

2.10.3.1 – Preparing the Disc

A disc prepared with the necessary reagents for the molybdenum blue method pre-dried onto it, as described in Figure 26, is to be used. There are ten channels which can be used to analyse samples. For the purposes of this study, two channels were used for the analysis of premade standards, one for a control measurement of deionized water, and seven for field samples.

To analyse a sample, a syringe or Eppendorf pipette was used to inject 300 μL of sample into the reaction well. The well was filled until a tiny air pocket remained around the

sample inlet. All samples were filtered the sample before injecting onto the disc to avoid clogging the micro-channels of the disc.

Once all of the samples have been added to the disc, it was gently shaken before waiting 10 minutes for the reaction to take place. After the reaction is complete, the disc was secured to the spindle and the analysis program was run (described in detail in Appendix 2, Section A2.3).

2.10.3.2 – Running a Test

After the test starts, the motor will bring the spindle up to speed and then spin it for the desired spin duration. Once the spin sequence is complete, the system will decelerate and then move to the first testing location. After each reading, the LED screen will display the readings for that well at the wavelength of 880 nm (the ideal wavelength for analysis of the molybdenum complex as discussed in Section 3.3) and save the full reading profile as a .TXT file on the SD card housed within the system.

2.10.3.3 – Extracting the Data and Analysis

Once all runs were complete, the data on the SD card was extracted to a computer for analysis within Excel. Within the .TXT file, the system saves information on the date and time the test began and the integration time used. Each well is saved written on a separate line with the first cell stating the corresponding well number and the result of the reading at the pixel for the 880 nm wavelength.

For analysis in this thesis, the data was extracted from the .TXT file and organized in columns within a pre-developed Excel spreadsheet. For more details on extracting the data and the system formatting of the data, refer to Appendix 2, Section A2.4.

2.11 Conclusion

This chapter describes the development of a portable, complete, analytical system for the on-site detection of phosphate in freshwater systems. The molybdenum blue method was optimised for the detection of P after being dried onto a surface, and a new microfluidic disc suitable for use with the molybdenum blue method and a vertical spectrometer detection system was developed. The Phosphasense Complete system was created, and an operating procedure was devised to allow for easy operation.

**Chapter 3: Evaluation of the PhosphaSense_MicroS_D2 System
for Multisite, Phosphate Catchment Monitoring**

3.1 Introduction

As discussed in Section 1, there is a need for a complete, portable, analytical system for the analysis of phosphate on site. The Phosphaload system developed by Joyce O’Grady⁴³ was a good stepping stone towards fulfilling this need. However, due to poor reproducibility between discs due to the manufacturing process, significant improvements were required for improved cross-disc reproducibility and precision. A comparison of the original Phosphaload system and the newer PhosphaSense_MicroS_D2 system is shown in Table 5.⁵

The main advantage of the PhosphaSense_MicroS_D2 system is that it is a *complete* analytical system. It enables the analysis of a sample as well as real-time comparison to predetermined standards alongside blanking all of the samples for a consistent baseline. The ability to do these measurements without needing to send the samples to the laboratory will enable faster monitoring for P and real time analysis. One of the main drawbacks of this system compared to its benchtop counterparts is that this system does require manual sampling and manual sample introduction, whereas in lab measurements can be automated.

3.2. Aims and Objectives

The aim of this chapter is to prove the precision, reproducibility, and deployability of PhosphaSense_MicroS_D2 system under controlled and field conditions. To fulfil this aim, the objectives are (1) validate the PhosphaSense_MiniS_D1 and PhosphaSense_MicroS_D2 using calibration lines encompassing the detection limits set

by the I-EPA, (2) calculate the LOD and LOQ of the PhosphaSense_MicroS_D2, (3) and perform field measurements with the PhosphaSense_MicroS_D2 at the catchment site.

3.3 Molybdenum Blue Method (solution and dried)

3.3.1 – Theory behind the Molybdenum Blue Method

The molybdenum blue method, also known as the ascorbic acid method, is a reaction where ammonium molybdate and potassium antimonyl tartrate react in a low pH environment to form a heteropoly acid in the presence of orthophosphate. This acid, specifically phosphomolybdic acid, is then reduced by ascorbic acid and turns the solution blue (outlined in Figure 24) which is best analysed at 880 nm⁵⁶. The intensity of the blue colour produced is dependent on the amount of orthophosphate present with the colour being more intense when more phosphate is in the sample, as demonstrated in Figure 25.²⁹ The reaction between ortho-P ions and molybdenum is optimized under highly acidic conditions (pH 0-1) in order to achieve the best colour intensity and stability⁵⁷⁻⁵⁹. Despite these highly acidic conditions, the concentrations of the acids used are low enough that it will not affect the plastics used in the design of the disc.

Known interferences for this method are few and listed are in Table 3 in Chapter 1. The only interferent known which can cause a reaction similar to that of phosphate with the molybdenum blue method are with arsenates at concentrations as low as 0.1 mg As/L. Hexavalent chromium and nitrogen dioxide can cause a reduction in the intensity of the colour change at concentrations as low as 1 mg/L.

According to literature, the reported approximate minimum concentration detectable is 10 µg P/L. The I-EPA has set the benchmark for high and good ecological status in fresh

waterbodies between 25 and 35 $\mu\text{g P/L}$ as benchmarks respectively (described further in Table 2).⁶

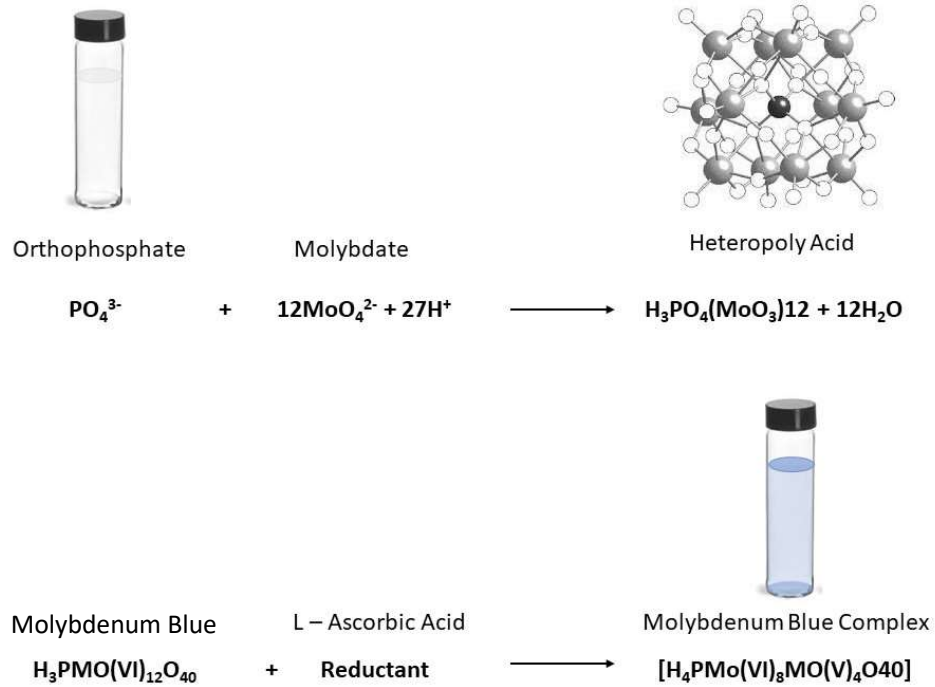


Figure 24: Illustration of molybdenum blue reaction in the presence of water sample with ortho-phosphate ions as analytes. This reaction forms a coloured molybdenum blue complex.



Figure 25: A single microfluidic disc with a concentration range of 0 - 50 $\mu\text{g P/L}$. Well 0 is 0 $\mu\text{g P/L}$, and well 1 is 50 $\mu\text{g P/L}$. The darker the colour of the reaction, the higher the P concentration.

The major drawback with this method is that once the reagents are combined in solution, they have a lifetime of 4 hours, which makes extending the lifetime of the assay of extreme importance. Ascorbic acid is the most unstable component of the reaction, which has a lifetime of 1 week when isolated and dried and is considered the limiting factor in this combined reagent.²⁹

3.3.2 – Molybdenum Blue Solution Method

The method used for the chemistry on the discs is an adapted version of the molybdenum blue method²⁹, which was refined and used by Joyce O'Grady *et al.* for the analysis of phosphate⁴³. It utilizes the combined reagents of 3.75 M sodium bisulphate (SB), 0.004 M potassium antimonyl tartrate hydrate (K-Tart.), 0.032 M ammonium molybdate tetrahydrate (AMT), and 0.1 M L-ascorbic acid (L-AA). For a cuvette with a sample volume of 3.5 mL, 0.56 mL of the combined reagent solution was added to 2.94 mL of analyte.

When doing analysis for the molybdenum blue solution method, all reagents were combined into a stock solution of the combined reagents prior to mixing with the analyte. A stock solution of 20 mL was prepared with the following quantities: 10 mL SB, 1 mL K-tart., 3 mL AMT, and 6 mL L-AA. Between the addition of each reagent, the reagents were mixed lightly by shaking the vial by hand. Upon completion of mixing the combined reagent, the solution should be pale yellow in colour.

3.3.3 – Dried Molybdenum Blue Method

For analysis using the molybdenum blue method dried on the microfluidic discs, the reagents were added to the disc in two distinct groups using Eppendorf pipettes atop an

exposed PSA layer: 3 of the reagents dried on the left side of the well, and one on the right side, as is shown in Figure 26. The separation of L-AA from the other reagents prevented the colorimetric change from taking place until the analyte was added. Due to a sample size of 300 μL for the well, the following quantities of each reagent were used: 16 μL SB, 4.8 μL K-Tart., 1.6 μL AMT, and 9.6 μL of L-AA.

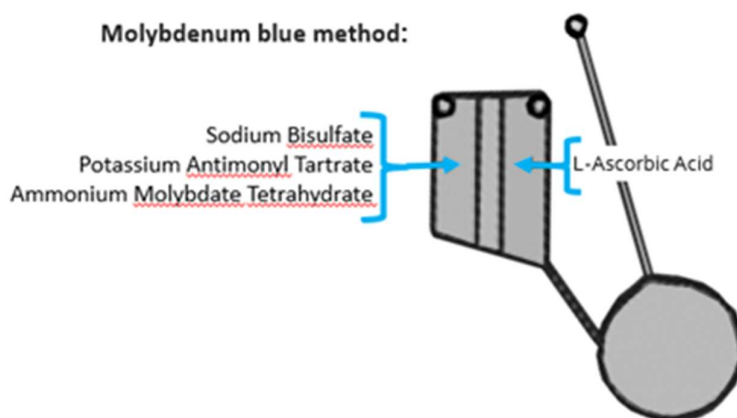


Figure 26: Distribution of combined reagent components within disc well

Once the reagents were dispensed onto the disc, it was placed into an oven that was preheated to 40 °C and dried for 1.5 hrs or until all droplets of the reagent were solid/crystallized in appearance.

3.4 Lab-based validation data for PhosphaSense Complete

3.4.1 – Validation of PhosphaSense_MiniS_D1

To validate the effectiveness of the combined reagent, standards of Potassium Phosphate Monobasic were used to create a calibration line (as is discussed further below). Due to the quantitative nature of the molybdenum blue method, a visible and quantifiable calibration curves were developed (as shown in Figures 27, 28 and 29).

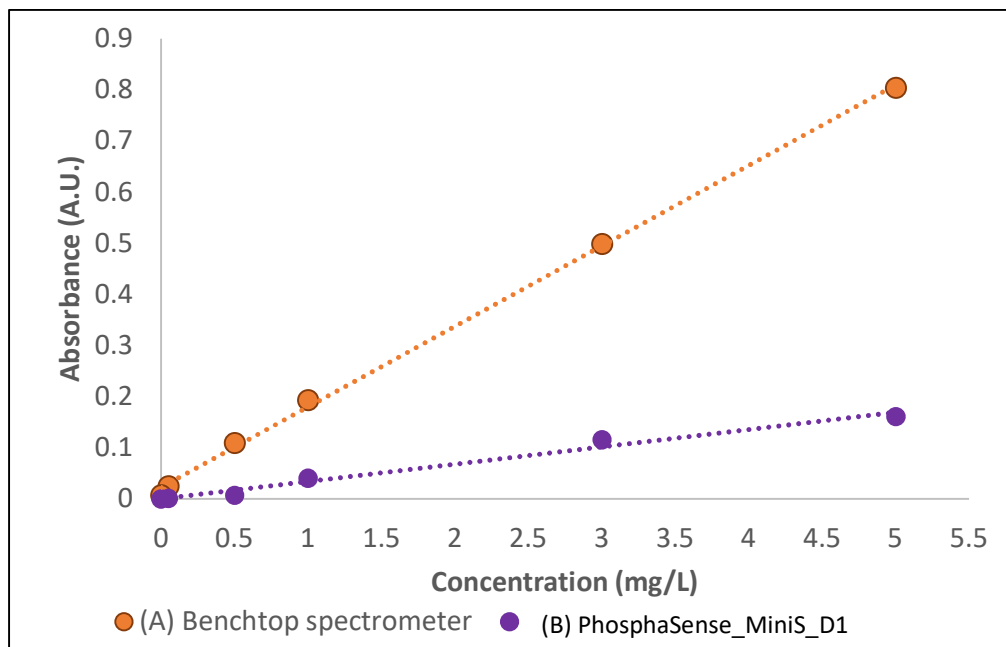


Figure 27: Calibration range comparing PhosphaSense_MiniS_D1 to a benchtop spectrometer. Calibration range: 0 – 5 mg/L; wavelength = 880 nm (A) n = 3, %RSD range 0.1 – 7. Equation of the Line: $y = 0.1574x + 0.0225$; $R^2 = 0.9989$. (B) n = 1; Equation of the Line: $y = 0.0338x + 0.003$; $R^2 = 0.9826$.

Figure 27 shows a comparison of the calibration curve of the PhosphaSense_MiniS_D1 system shown in Figure 7 and the UVmini-1240 Shimadzu benchtop spectrometer along the range of 0 – 5 mg P/L (0 – 5,000 μ g P/L). The reproducibility of the two methods on this system were very comparable: with the benchtop having a %RSD of 0.4 and the PhosphaSense_MiniS_D1 having a %RSD of 0.7. The major difference observed was that while the intensity of the absorbance observed was approximately 0.2 A.U. lower for the PhosphaSense_MiniS_D1 than the benchtop system.

Next, a series of experiments testing the reproducibility of the measurements was conducted. In this experiment, the calibration standard of 3 mg/L was measured five times at the wavelength of 880 nm. The %RSD for the five measurements was 0.7 with an average absorbance of 0.303 A.U.. For comparison, the same experiment was carried out on the benchtop spectrometer. The benchtop system achieved a %RSD of 0.4 and an

average absorbance of 0.499 A.U.. These two series of experiments prove that the first iteration of the PhosphaSense_MiniS_D1 to be comparative to the benchtop system.

3.4.2 – Validation of PhosphaSense_MicroS_D2

After the applicability of a mini-spectrometer for the detection of phosphate via the molybdenum blue method was proven, a C12880MA micro-spectrometer was installed into the PhosphaSense_MicroS_D2 system and evaluated using similar tests as those described in Section 3.4.1.

The micro-spectrometer in the PhosphaSense_MicroS_D2 system produced reliable and repeatable calibration curves, similar to those produced by the PhosphaSense_MiniS_D1. Figures 28 and 29 show examples of one of the initial trials. This study analysed both the precision and the reproducibility of the system. To achieve this, three identical discs were assembled with two replicates of each standard per disc across a range of 0 to 500 $\mu\text{g P/L}$. Each disc was scanned three times with the PhosphaSense_MicroS_D2 system, enabling an analysis into the reproducibility per disc and across multiple discs.

Figure 28 shows the average of the 3 discs vs. the benchtop spectrometer system. Across three discs with three replicates per disc, the average %RSD was 2, and the benchtop system achieved a %RSD of 0.4 for three replicates. The low %RSD for a total of 9 replicates indicates a high level of precision for the microfluidic discs in the PhosphaSense_MicroS_D2 system compared to its benchtop counterpart.

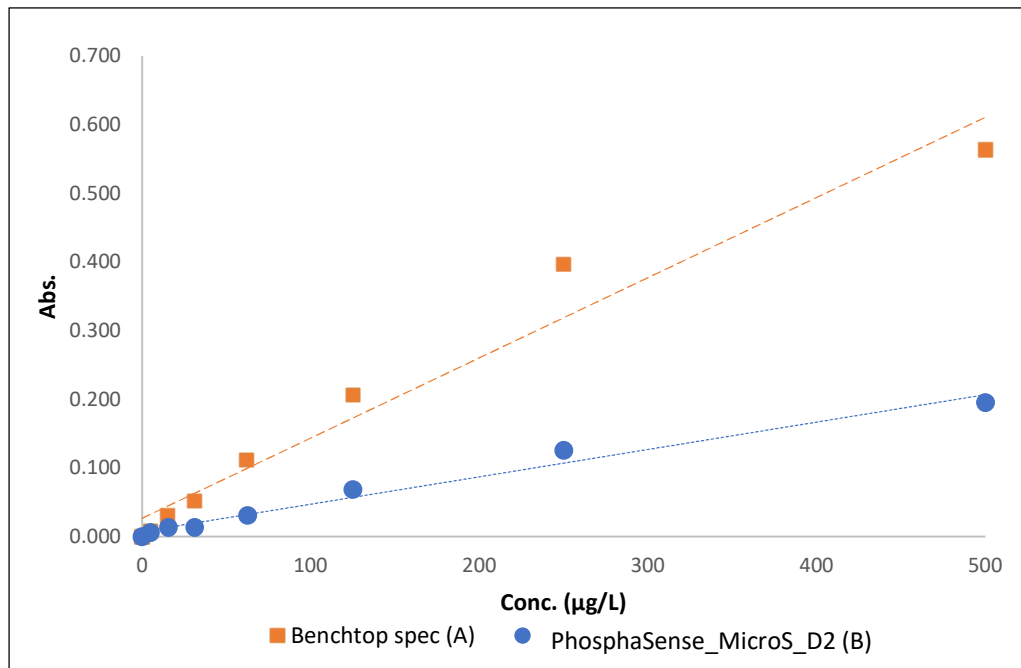


Figure 28: (A) The calibration curve for the laboratory spectrometer (UV-Vis mini – 1240 Shimadzu); wavelength of 880 nm; calibration range of 0 µg PO₄ /L to 500 µg P/L; n = 3; Average %RSD 0.4. Equation of the line: $y = 0.0012x + 0.0267$; $R^2 = 0.9626$. (B) PhosphaSense_MicroS_D1 System; wavelength 880.4 nm; calibration range of 0 µg P/L to 500 µg P/L; integration time = 0.0001; $n_{\text{well}} = 3$; number of wells per concentration = 2; Average %RSD 2. Equation of the Line: $y = 0.0004x + 0.0073$; $R^2 = 0.979$.

The data was then broken down to study the response of each individual disc and to compare their responses. Individually, each disc had a low %RSD: 1.0, 0.6, and 0.5 for discs 1 through 3 respectively. It can also be observed that all of the responses are extremely close in intensity, with less than a 0.1 A.U. difference between the farthest data points, and several directly overlap with each other. This further demonstrates the precision of the PhosphaSense_MicroS_D2 system across a single disc and multiple discs.

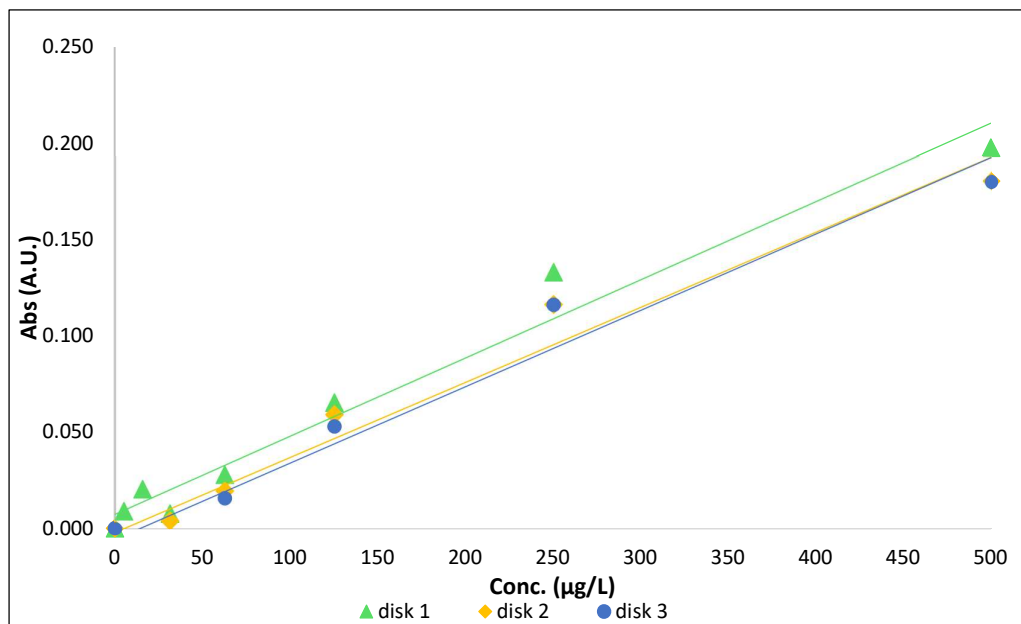


Figure 29: Calibration curve with a range of 0 µg P/L to 500 µg P/L demonstrating the reproducibility of the PhosphaSense_MicroS_D2. LED wavelength = 880 nm; integration time = 0.0001; $n_{\text{well}} = 3$; number of wells per concentration = 1; Average % RSD = 0.7. Disc 1: equation of the line: $y = 0.004x + 0.0078$; $R^2 = 0.9698$. Disc 2: equation of the line: $y = 0.0004x - 0.0017$; $R^2 = 0.9733$. Disc 3: equation of the line: $y = 0.0004x - 0.0055$; $R^2 = 0.9715$.

3.5 Determination of LOD and LOQ

After the data discussed above was collected, the LOD and LOQ of the PhosphaSense_MicroS_D2 using the calibration data shown in Figure 28 was calculated. The equations used to calculate the LOD and LOQ are as follows:

Equation 1: Limit of Detection

$$LOD = \frac{\sigma}{S} \times 3.3$$

Equation 2: Limit of Quantification

$$LOQ = \frac{\sigma}{S} \times 10$$

where σ = the standard deviation of the response and S = the slope of the calibration curve. The standard deviation was calculated from the standard error using the following equation:

Equation 3: Calculating Standard Deviation from Standard Error

$$\sigma = SE \times \sqrt{N}$$

Where SE is the standard error, calculated using the LINSET function within Excel, and N is the number of replicates/samples. In this case, N = 9.

Table 7 details the results from the equations listed above. Based on the results calculated, with an LOQ of 3.4 $\mu\text{g P/L}$, the PhosphaSense_MicroS_D2 system is capable of quantifying samples within the ranges of 25 and 35 $\mu\text{g P/L}$ set by the I-EPA for ideal P limits in freshwater lakes and rivers.

Table 7: LOD and LOQ of PhosphaSense_MicroS_D2 systems

System	σ	S	LOD ($\mu\text{g P/L}$)	LOQ ($\mu\text{g P/L}$)
PhosphaSense_MicroS_D2	0.000136	0.000396	1.3	3.4

3.6 Description of Field Sites

Sample sites for testing the applicability of the system in the field were found using the EPA maps webpage⁶⁰ with the National Water Monitoring Stations filter. The three specific sites were selected for their ease of access along the Maiden River in Tubbercurry, Ireland: RS34T030300, RS34T020050, and RS34T020100.

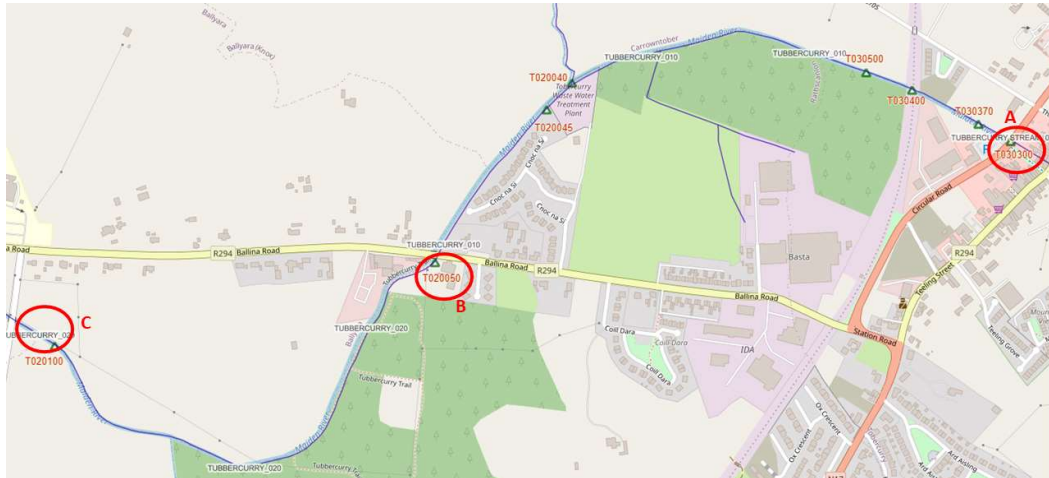


Figure 30: Map of sampling sites along the Maiden River in Tubbercurry, Co. Sligo, Ireland.⁶⁰

The first site (Site A), near monitoring station RS34T030300, was located at the corner of a SuperValu parking lot and the west side of the N17 Bridge which runs through the Tubbercurry (coordinates: 54° 03' 15.7" N and 8° 43' 52.9" W). Figure 31 Shows the exact location of sampling facing the N17 Bridge, which is accessible from the parking lot.



Figure 31: Field Site A, Monitoring Station T030300. Location: 54° 03' 15.7" N and 8° 43' 52.9" W

Field site B, near monitoring station RS34T020050, was located next to the parking lot for the Forest Trail hiking path in Tubbercurry, just south of the bridge for R294 over the Maiden River. (coordinates: 54° 03' 08.2"N and 8° 44' 52.2"W). Figure 32 Shows the location of sampling facing the bridge, which is accessible from the parking lot or with a bucket from the bridge.



Figure 32: Field site B, Monitoring Station T020050. Location: 54° 03' 08.2"N and 8° 44' 52.2"W

The final sampling site (field site C) was located near monitoring station RS34T020100. The monitoring station is in a field on the east side of Ballina Road, Tubbercurry. Due to the monitoring station being adjacent to private property, the sampling location was just east of the bridge crossing the Maiden River for Ballina Road (coordinates: 54° 03' 04.5" N and 8° 45' 35.1" W). Figure 33 shows the location facing north on the east side of the bridge, which is accessible from the road with a bucket from the bridge.



Figure 33: Field site B, near Monitoring Station T020100. Location: 54° 03' 04.5" N and 8° 45' 35.1" W

3.7 Field testing results

To field test the Phosphasense system, it was taken to three sites in Tubbercurry, Sligo, Ireland in February of 2023. A listing of these sites and images of them can be found in Section 3.6. The weather prior to sampling had been light showers of rain throughout the day, and the water levels were lower than observed previously. Alongside phosphate concentration, measurements of the temperature, pH, conductivity, and dissolved oxygen content (DOC) were taken on site. For phosphate analysis, each location was sampled in three wells and repeated on two discs, meaning each sample was measured six times in total. All results are shown in Table 8 below. All sites were selected because they are near EPA water monitoring stations (WMS) in areas which were being surveyed for phosphorous levels.⁶⁰

Site A is the eastern most sampling points along the Maiden River and the most upstream. It is also the closest point to the town centre. The river runs under the main road through the town, and travels underground before reaching the sampling point. On the north-east side of the site is a field, and on the south-west side is a parking lot. To the south-east is the main road (N17) and to the north-west are fields and some forest. The P concentration for this site was found to be 12.1 µg/L, with is within the LOQ limit.

Site B is located on the western edge of Tubbercurry and is downstream of a wastewater treatment plant and housing development. To the west are fields and to the east is the town of Tubbercurry itself. Visually, the water at Site B was very similar to Site A, but it had a slightly higher P concentration of 19.6 µg/L, but a slightly lower conductivity and DOC than Site A.

The final site, Site C, is located on the west side outskirts of Tubbercurry, surrounded on all sides by fields/pastures. The water here was more coloured than in the previous two locations, having a brown tint to it, and it had the highest conductivity, pH, and the DOC of the three sites. However, despite having higher readings for all of these parameters compared to the other sampling sites, it had a P concentration of 16.4 µg/L.

Table 8: Summarization of Data for Field Testing of Phosphasense in Tubbercurry, Ireland.

Location/ WMS	Water Colour	Conc. P (μg P/L)	Temp. ($^{\circ}\text{C}$)	pH	Conductivity	DOC	Water Quality according to I-EPA
A RS34T030300	Clear	12.1	10.2	7.55	472	9.08 mg/L	Good
						82.30%	
B RS34T020050	Very Faint Colour	19.6	9.7	7.59	442	8.67 mg/L	Good
						76.90%	
C RS34T020100	Coloured	16.4	9.7	7.70	456	9.37 mg/L	Good
						83.20%	

During deployment, the system proved easy to use, with the running of the system being the same as when analysing standards in the lab (discussed in Section 3.4.2). Closing of the lid during runs prevented interference from changing light conditions in the environment. Each test took fifteen minutes to complete per run, so with three runs per disc, the total run time for one disc was forty-five minutes.

Replicates of the samples were run both on one disc and across multiple discs. Similar to when calibration tests were being conducted, each sample site was deposited into two separate wells per disc. This was then repeated on another disc to study the measurement repeatability.

Due to circumstances beyond the author's control during this study and the 48 hour lifespan of P samples²⁹, a benchtop comparison of the samples in Table 8 could not be performed. Three other sampling trips were conducted over the next four months, but didn't yield any usable data for the following reasons:

- Sampling Trip 2: Contamination on the discs due to contamination in the oven used to dry the reagents onto the disc. This contamination caused the control (DI water) to turn blue, and therefore the data was considered unusable.
- Sampling Trip 3: the calibration samples were acceptable for this trip and the contamination issue from Trip 2 was resolved by changing ovens, but the field samples were taken towards the end of an extreme flooding event and no phosphate was detected. Discussions between members of the team speculated that much of the phosphate had already been washed away by the time it was possible to go sampling.
- Sampling Trip 4: Forecasts called for rain after a long dry spell in the summer. On the day chosen for sample collection, light and sporadic showers happened instead of the heavier rain anticipated. This meant that phosphorous levels were too low to detect on both the benchtop system and the PhosphaSense_MicroS_D2.

Because the sampling site was a 5 hour round trip by train, future testing sites should be closer to the laboratory so more frequent testing can be conducted more easily.

3.8 Conclusion

The Phosphasense Complete system has demonstrated the ability to be a complete, portable, analytical system for the detection of phosphate. Trials in the laboratory and the field have been conducted, and demonstrate the system's reliable reproducibility, an improvement from the original Phosphaload system, and its ability to quantify P at low concentrations (between 12.1 – 19.6 µg/L) using the molybdenum blue method. To achieve this, various iterations of microfluidic discs were designed until the optimal configuration was determined and optimised. A version of the molybdenum blue method using dried on-a-disc reagents was optimized enabling the detection of phosphate outside of the laboratory. This novel micro-spectrometer based analyser was then deployed at various sites around Tubbercurry, Sligo and was able to successfully detect P at the catchment.

Chapter 4: Overall Conclusions

4.1 Conclusion

The aim of this project was to develop a complete, analytical P detection system capable of doing real time phosphate analysis at the catchment site. The ability to detect P at the catchment site in order to monitor the effects of weather events is becoming increasingly important as climate change continues to cause changes in precipitation, temperature, and erosion. These changes affect the amount of P which can be found in soils and in the freshwater systems. Therefore, the PhosphaSense Complete system will be able to detect P within the range of the legislation outlined as by the I-EPA for good ecological status. However, the type of monitoring this system provides is inherently limited by the need to have personnel on-site for sampling and testing. Therefore, the amount of testing/analysis which can be performed, or locations which can be analysed, is limited by the number of personnel available.

The system developed has proven that it is capable of producing linear calibration curves with R^2 ranges averaging above 0.97 and high levels of precision with an average %RSD of 2.7, an LOD of 1.3 $\mu\text{g P/L}$, and an LOQ of 3.4 $\mu\text{g P/L}$. The system has also proven its ability to produce repeatable measurements both across wells on a singular disc and across multiple discs, which is an improvement upon the original Phosphaload_DP_2021 system where reproducibility was limited on a per disc basis. With a weight of 3 kg, a robust chemical method, and the ability to run 10 samples per disc, the PhosphaSense_MicroS_D2 system is a complete, analytical system which can be taken to and run in the field.

To demonstrate this, it was deployed in three locations along the Maiden River in Tubbercurry, Sligo, Ireland. The system was able to successfully detect levels of

phosphate between 12 and 19 µg/L, proving its ability to be used in the field and easily deployed outside of laboratory conditions.

4.2 Future Work

While the Phosphasense Complete is a complete analytical system, there is still some work to be done which can improve it further. The first thing which could be expanded upon is working to extend the shelf-life of the discs. Based on the research conducted by Joyce O'Grady, the reagents on the discs have a shelf-life of one week⁴³, however, there are options which have the potential to extend that lifetime. Some of these options include: vacuum sealing the disc with a desiccator pack inside the bag alongside the disc and flooding the vacuum bag with a neutral gas before sealing it.

Another thing which can evaluate the effectiveness of the system would be more field deployments of the system in a wider range of locations. This may further prove its applicability and potential in a variety of conditions. Finally, the system should be distributed to various user groups, such as partner research teams evaluating water quality and Teagasc, to demonstrate the ease of use of the system and the level of training required to operate the system appropriately.

Finally, a study into using this system for the detection of other nutrients which are of concern in freshwater systems, such as nitrates and nitrites, would be advantageous in making this system an even more versatile analytical instrument. The ability to detect multiple nutrients on site with a singular, easy to use system would be revolutionary in the water monitoring community and allow for real time and rapid decision making during constantly changing weather events.

5.0 References

- (1) Kristensen, P. *Nutrients in Freshwater in Europe*; Indicator; European Environment Agency, 2020. <https://www.eea.europa.eu/data-and-maps/indicators/nutrients-in-freshwater> (accessed 2023-09-27).
- (2) M Biddulph; Collins, A. L.; Foster, I. D. L.; Holmes, N. The Scale Problem in Tackling Diffuse Water Pollution from Agriculture: Insights from the Avon Demonstration Test Catchment Programme in England. *River Res. Appl.* **2017**, *33* (10), 1527–1538. <https://doi.org/10.1002/rra.3222>.
- (3) EEA. *European Waters -- Assessment of Status and Pressures 2018 — European Environment Agency*. <https://www.eea.europa.eu/publications/state-of-water> (accessed 2022-06-13).
- (4) European Environment Agency. *Phosphorus in lakes and rivers - Nutrient trends in European water bodies*. https://www.eea.europa.eu/data-and-maps/daviz/phosphorus-in-lakes-and-rivers-2#tab-googlechartid_googlechartid_chart_111 (accessed 2023-09-27).
- (5) O’Grady, J.; Kent, N.; Regan, F. Design, Build and Demonstration of a Fast, Reliable Portable Phosphate Field Analyser. *Case Stud. Chem. Environ. Eng.* **2021**, *4*, 100168. <https://doi.org/10.1016/j.cscee.2021.100168>.
- (6) Irish EPA. *Water Quality in 2022: An Indicators Report*; EPA, 2023; p 9. <https://www.epa.ie/publications/monitoring--assessment/freshwater--marine/Water-Quality-2022-Indicator-Report-Web.pdf> (accessed 2023-09-17).
- (7) European Environment Agency. *Ecological status of surface waters in Europe*. <https://www.eea.europa.eu/ims/ecological-status-of-surface-waters> (accessed 2023-07-17).
- (8) Carvalho, L.; McDonald, C.; de Hayos, C.; Mischke, U.; Phillips, G.; Borics, G. Sustaining Recreational Quality of European Lakes: Minimizing the Health Risks from Algal Blooms through Phosphorus Control. *J Appl Ecol* **2013**, *50* (2), 315–332.
- (9) Bol, R.; Gruau, G.; Mellander, P.-E.; Dupas, R.; Bechmann, M.; Skarbøvik, E.; Bieroza, M.; Djodjic, F.; Glendell, M.; Jordan, P.; Van der Grift, B.; Rode, M.; Smolders, E.; Verbeeck, M.; Gu, S.; Klumpp, E.; Pohle, I.; Fresne, M.; Gascuel-Oudou, C. Challenges of Reducing Phosphorus Based Water Eutrophication in the Agricultural Landscapes of Northwest Europe. *Front. Mar. Sci.* **2018**, *5* (276), 1–17. <https://doi.org/10.3389/fmars.2018.00276>.
- (10) Berg, M.; Meehan, M.; Franzen, D.; Scherer, T. *Phosphorus Behavior in the Environment*. North Dakota State University: Publications. <https://www.ag.ndsu.edu/PUBLICATIONS/environment-natural-resources/phosphorus-behavior-in-the-environment#:~:text=The%20forms%20of%20phosphorus%20present,can%20move%20within%20the%20environment.> (accessed 2023-11-03).
- (11) Julien, N. *Phosphorus and eutrophication*. https://www.encyclopedie-environnement.org/en/water/phosphorus-and-eutrophication/#4_Excess_phosphorus_and_eutrophication (accessed 2023-10-06).
- (12) Bergström, L.; Kirchmann, H.; Djodjic, F.; Kyllmar, K.; Ulén, B.; Liu, J.; Andersson, H.; Aronsson, H.; Börjesson, G.; Kynkäänniemi, P.; Svanbäck, A.; Villa, A. Turnover

- and Losses of Phosphorus in Swedish Agricultural Soils: Long-Term Changes, Leaching Trends, and Mitigation Measures. *J. Environ. Qual.* **2015**, *44*, 512–523.
- (13) Duffy, G.; Regan, F. Recent Developments in Sensing Methods for Eutrophying Nutrients with a Focus on Automation for Environmental Applications. *Analyst* **2017**, *142*, 4355–4372. <https://doi.org/10.1039/c7an00840f>.
- (14) Chen, H.; Zhao, L.; Yu, F.; Du, Q. Detection of Phosphorus Species in Water: Technology and Strategies. *Analyst* **2019**, No. 24. <https://doi.org/10.1039/C9AN01161G>.
- (15) Environment and Climate Change Canada (ECCC). *Partnering on Achieving Phosphorus Loading Reductions to Lake Erie from Canadian Sources*. <https://www.canada.ca/en/environment-climate-change/services/great-lakes-protection/action-plan-reduce-phosphorus-lake-erie.html#toc44> (accessed 2023-12-22).
- (16) Alliance for the Great Lakes. *Lake Erie Algae Blooms*. <https://greatlakes.org/campaigns/lake-erie-algae-blooms/> (accessed 2023-12-22).
- (17) Schoumans, O. F.; Bouraoui, F.; Kabbe, C.; Oenema, O.; van Dijk, K. C. Phosphorus Management in Europe in a Changing World. *AMBIO* **2015**, *44*, S180–S192. <https://doi.org/10.1007/s13280-014-0613-9>.
- (18) Prasad, R.; Chakraborty, D. *Phosphorus Basics: Understanding Phosphorus Forms and Their Cycling in the Soil*. Extension: Alabama A&M Auburn Universities. <https://www.aces.edu/blog/topics/crop-production/understanding-phosphorus-forms-and-their-cycling-in-the-soil/> (accessed 2023-11-03).
- (19) Ziadi, N.; Whalen, J. K.; Messiga, A. J.; Morel, C. *Advances In Agronomy*; Elsevier: Burlington, 2013; Vol. 112.
- (20) MET Eireann. *Rainfall: Rainfall Climate of Ireland*. Rainfall. <https://www.met.ie/climate/what-we-measure/rainfall> (accessed 2023-10-06).
- (21) Moloney, T.; Fenton, O.; Daly, K. Ranking Connectivity Risk for Phosphorus Loss along Agricultural Drainage Ditches. *Sci. Total Environ.* **2020**, *703*, 134556. <https://doi.org/10.1016/j.scitotenv.2019.134556>.
- (22) Lee, H.; Romero, J.; Core Writing Team, I. *Climate Change 2023 Synthesis Report Summary*; Intergovernmental Panel on Climate Change: Geneva, Switzerland, 2023. https://www.ipcc.ch/report/ar6/syr/downloads/report/IPCC_AR6_SYR_SPM.pdf (accessed 2023-10-17).
- (23) Irish EPA. *Summary Report: Water Quality in Ireland 2016-2021*; Summary Report; EPA.IE: Wexford, Ireland, 2021. https://www.epa.ie/publications/monitoring--assessment/freshwater--marine/WaterQuality_SummaryReport.pdf (accessed 2023-11-03).
- (24) Ezzati, G.; Fenton, O.; Healy, M. G.; Christianson, L.; Feyereisen, G. W.; Thornton, S.; Chen, Q.; Fan, B.; Ding, J.; Daly, K. Impact of P Inputs on Source-Sink P Dynamics of Sediment along an Agricultural Ditch Network. *J. Environ. Manage.* **2020**, *257* (109988), 1–11. <https://doi.org/10.1016/j.jenvman.2019.109988>.
- (25) Environmental Protection Agency, Ireland. *Water Quality Monitoring Report on Nitrogen and Phosphorus Concentrations in Irish Waters 2021*; annual; EPA.IE, 2022. www.epa.ie/publications/monitoring--assessment/freshwater--marine/EPA_NitrogenandPhosphorous_Concentrations_2021.pdf (accessed 2023-09-28).

- (26) Litke, D. W. *Review of Phosphorus Control Measures in the United States and Their Effects on Water Quality*; U.S. Geological Survey; Water-Resources Investigations 99-4007; National Water-Quality Assessment Program: Denver, Colorado, 1999; pp 1-43.
- (27) Poikane, S.; Kelly, M. G.; Herrero, F. S.; Pitt, J.-A.; Jarvie, H. P.; Claussen, U.; Leujak, W.; Solheim, A. L.; Teixeira, H.; Phillips, G. Nutrient Criteria for Surface Waters under the European Water Framework Directive: Current State-of-the-Art, Challenges, and Future Outlook. *Sci. Total Environ.* **2019**, *695*, 133888. <https://doi.org/10.1016/j.scitotenv.2019.133888>.
- (28) Australian Government: Department of Climate Change, Energy, the Environment and Water. *Total Phosphorus*. <https://www.dcceew.gov.au/environment/protection/npi/substances/fact-sheets/total-phosphorus> (accessed 2023-09-28).
- (29) *Standard Methods for the Examination of Water and Wastewater Parts 1 and 2*; Standard methods; American Public Health Association, American Water Works Association, Water Environment Federation: USA, 1999; pp 1-541,1-733.
- (30) Zhu, X.; Ma, J. Recent Advances in the Determination of Phosphate in Environmental Water Samples: Insights from Practical Perspectives. *Trends Anal. Chem.* **2020**, *127*, 1-16. <https://doi.org/10.1016/j.trac.2020.115908>.
- (31) Alam, M. M.; Srinivasan, V.; Mueller, A. V. Status and Advances in Technologies for Phosphorus Species Detection and Characterization in Natural Environment - A Comprehensive Review. *Talanta* **2021**, *233*. <https://doi.org/10.1016/j.talanta.2021.122458>.
- (32) Stauffer, R. E. Determination of Arsenic and Phosphorus Compounds in Groundwater with Reduced Molybdenum Blue. *Anal. Chem.* **1983**, *55* (8).
- (33) Oliveira, E. M.; Rogero, M.; Ferreira, E. C.; Neto, J. A. G. Simultaneous Determination of Phosphite and Phosphate in Fertilizers by Raman Spectroscopy. *Spectrochim. Acta. A. Mol. Biomol. Spectrosc.* **2021**, *246*. <https://doi.org/10.1016/j.saa.2020.119025>.
- (34) Duffy, G.; Maguire, I.; Heery, B.; Nwankire, C.; Ducreé, J.; Regan, F. PhosphaSense: A Fully Integrated, Portable Lab-on-a-Disc Device for Phosphate Determination in Water. *Sens. Actuators B Chem.* **2017**, *246*, 1085-1091. <https://doi.org/10.1016/j.snb.2016.12.040>.
- (35) *Development of a Portable In Situ Phosphorous Sensor*; Technical Report DOE-ExMat-WSU-SC0022391; ExMat Research, Inc.: Spokane, WA, 2023. <https://www.osti.gov/biblio/1958102> (accessed 2023-09-29).
- (36) Ryan, K. A.; Palacios, L. C.; Encina, F.; Graeber, D.; Osorio, S.; Stubbins, A.; Woelfl, S.; Nimptsch, J. Assessing Inputs of Aquaculture-Derived Nutrients to Streams Using Dissolved Organic Matter Fluorescence. *Sci. Total Environ.* **2022**, *807 Pt 2*. <https://doi.org/10.1016/j.scitotenv.2021.150785>.
- (37) Chelsea Technologies. *UviLux Tryptophan*. <https://chelsea.co.uk/products/uvilux-tryptophan/#main> (accessed 2023-10-07).
- (38) Lin, B.; Xu, J.; Lin, K.; Li, M.; Lu, M. Low-Cost Automatic Sensor for in Situ Colorimetric Detection of Phosphate and Nitrate in Agricultural Water. *ACS Sens.* **3** (12). <https://doi.org/10.1021/acssensors.8b00781>.

- (39) Precision Laboratories. *Phosphate Test Strip*. <https://www.prelaboratories.com/product/phosphate-test-strip/> (accessed 2023-10-06).
- (40) Li, Z.; Liu, H.; Wang, D.; Zhang, M.; Yang, Y.; Ren, T. Recent Advances in Microfluidic Sensors for Nutrients Detection in Water. *TrAC Trends Anal. Chem.* **2022**, *158*. <https://doi.org/10.1016/j.trac.2022.116790>.
- (41) Cleary, J.; Maher, D.; Slater, C.; Diamond, D. In Situ Monitoring of Environmental Water Quality Using an Autonomous Microfluidic Sensor. *IEEE Sens. J.* **2014**. <https://doi.org/10.1109/SAS.2010.5439385>.
- (42) Grand, M. M.; Clinton-Bailey, G. S.; Beaton, A. D.; Schaap, A. M.; Johengen, T. H.; Tamburri, M. N.; Connelly, D. P.; Mowlem, M. C.; Achterberg, E. P. A Lab-On-Chip Phosphate Analyzer for Long-Term In Situ Monitoring at Fixed Observatories: Optimization and Performance Evaluation in Estuarine and Oligotrophic Coastal Waters. *Front. Mar. Sci.* **2017**, *4* (255). <https://doi.org/10.3389/fmars.2017.00255>.
- (43) O'Grady, J. Enabling near Real-Time Monitoring of Phosphate in Catchment Areas. Doctor of Philosophy, Dublin City University (DCU), Dublin, IE, 2021.
- (44) Su, P.-W.; Lo, S.-L. Using Landsat 8 Imagery for Remote Monitoring of Total Phosphorus as a Water Quality Parameter of Irrigation Ponds in Taiwan. **2021**. <https://doi.org/10.21203/rs.3.rs-231078/v1>.
- (45) Xiong, J.; Lin, C.; Ma, R.; Cao, Z. Remote Sensing Estimation of Lake Total Phosphorus Concentration Based on MODIS: A Case Study of Lake Hongze. *Remote Sens.* **2019**, *11*. <http://dx.doi.org/10.3390/rs11172068>.
- (46) Du, C.; Li, Y.; Lyu, H.; Naisen, L.; Zheng, Z.; Li, Y. Remote Estimation of Total Phosphorus Concentration in the Taihu Lake Using a Semi-Analytical Model. *Int. J. Remote Sens.* **2020**, *41* (20). <https://doi.org/10.1080/01431161.2020.1767826>.
- (47) Villa, A.; Folster, J.; Kyllmar, K. Determining Suspended Solids and Total Phosphorus from Turbidity Comparison of High-Frequency Sampling with Conventional Monitoring Methods. *Environ. Monit. Assess.* **2019**, *191* (605).
- (48) Kamari, M.; Tarvainen, M.; Kotamaki, N.; Tattari, S. High-Frequency Measured Turbidity as a Surrogate for Phosphorus in Boreal Zone Rivers: Appropriate Options and Critical Situations. *Environ. Monit. Assess.* **2020**, *192* (366). <https://doi.org/10.1007/s10661-020-08335-w>.
- (49) Castrillo, M.; Garcia, A. L. Estimation of High Frequency Nutrient Concentrations from Water Quality Surrogates Using Machine Learning Methods. *Water Res.* **2020**, *172*. <https://doi.org/10.1016/j.watres.2020.115490>.
- (50) Sivasankaran, U.; Reinke, L.; Anand, S. K.; Malecka, K.; Kumar, K. G.; Radecka, H.; Kubik, S.; Radecki, J. Ultrasensitive Electrochemical Sensing of Phosphate in Water Mediated by a Dipicolylamine-Zinc(II) Complex. *Sens. Actuators B Chem.* **2020**, *321*. <https://doi.org/10.1016/j.snb.2020.128474>.
- (51) Xu, K.; Li, Y.; Li, M. Potentiometric Phosphate Ion Sensor Based on Electrochemical Modified Tungsten Electrode. *ACS Omega* **2021**, *6* (21). <https://doi.org/10.1021/acsomega.1c00195>.
- (52) Adobe. *DWG files*. <https://www.adobe.com/ie/creativecloud/file-types/image/vector/dwg-file.html> (accessed 2023-09-26).
- (53) Adobe. *DWF files*. [https://www.adobe.com/creativecloud/file-](https://www.adobe.com/creativecloud/file-types/image/raster/dwf-)
[types/image/raster/dwf-](https://www.adobe.com/creativecloud/file-types/image/raster/dwf-)

- file.html#:~:text=DWF%20is%20short%20for%20Design,without%20any%20specialist%20software%20programs. (accessed 2023-09-26).
- (54) Profinet University. *Profinet GSD File Basics*.
<https://profinetuniversity.com/profinet-basics/profinet-gsd-file-basics/#:~:text=What%20is%20a%20GSD%20File,and%20vendor%20and%20device%20identification>. (accessed 2023-09-26).
- (55) Beggy, H. *Updating an Existing Phosphate Sensing System*; Undergraduate final year project; Dublin City University, 2022.
- (56) Baldwin, D. S. Reactive “Organic” Phosphorus Revisited. *Water Res.* **1998**, *32* (8), 2265–2270. [https://doi.org/10.1016/S0043-1354\(97\)00474-0](https://doi.org/10.1016/S0043-1354(97)00474-0).
- (57) Crouch, S. R.; Malmstadt, H. V. Mechanistic Investigation of Molybdenum Blue Method for Determination of Phosphate. *Anal. Chem.* **1967**, *39* (10), 1084–1089. <https://doi.org/10.1021/ac60254a027>.
- (58) Galhardo, C. X.; Masini, J. C. Spectrophotometric Determination of Phosphate and Silicate by Sequential Injection Using Molybdenum Blue Chemistry. *Anal. Chem. Acta* **2000**, *417* (2), 191–200. [https://doi.org/10.1016/S0003-2670\(00\)00933-8](https://doi.org/10.1016/S0003-2670(00)00933-8).
- (59) Nagul, E. A.; McKelvie, I. D.; Worsfold, P.; Kolev, S. D. The Molybdenum Blue Reaction for the Determination of Orthophosphate Revisited: Opening the Black Box. *Anal. Chem. Acta* **2015**, *890* (26), 60–82. <https://doi.org/10.1016/j.aca.2015.07.030>.
- (60) EPA Maps - National Water Monitoring Stations, 2023. <https://gis.epa.ie/EPAMaps/>.

Appendix 1: List of Poster and Oral Presentations

Oral Presentations

- European Geosciences Union General Assembly, Vienna, Austria (April 25, 2023)
- Environmental Services Association 2023 Researcher’s Colloquium, ATU Donegal, Ireland (April 4, 2023)
- International Water Association Diffuse Pollution & Eutrophication Conference (IWA DIPCON), Istanbul, Turkey (October 27, 2023)

Poster Presentations

- NCSR Research Day, Dublin City University, Ireland (June 16, 2022)
- Royal Society of Chemistry Analytical Research Forum, London, England (June 14, 2022)

Appendix 2: Operating PhosphaSense_MicroS_D2

A2.1. System Layout:

Phosphasense Complete is a simple system with three main components: the main body of the system itself (shown and detailed in Figure 34) the inner electrical components (shown and detailed in Figure 35) and the microfluidic disc (shown and detailed in Figure 19).

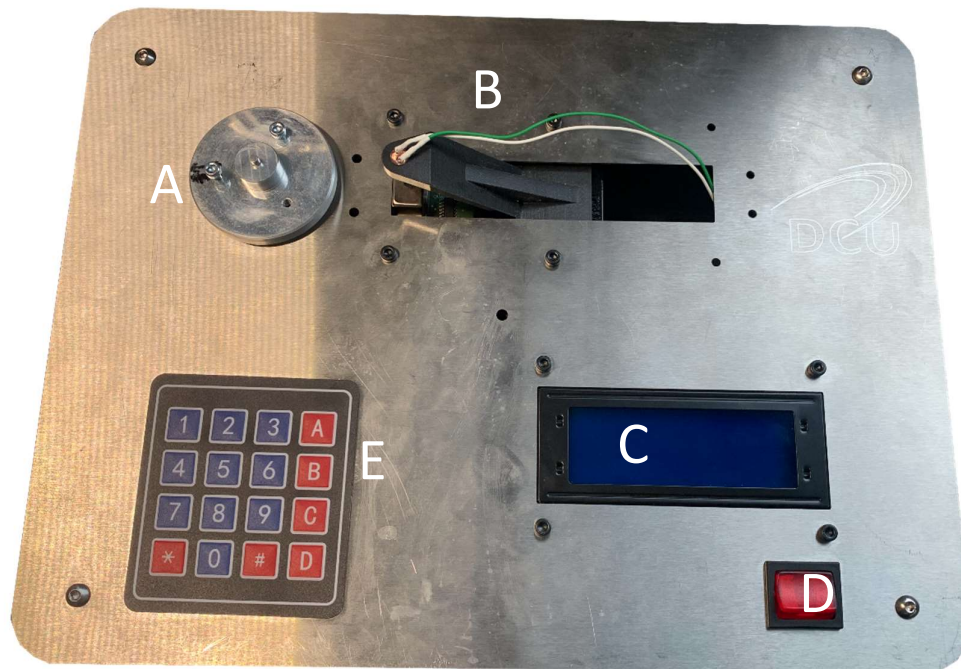


Figure 34: Layout of main body of the system. (A) Spindle/Disc mount, (B) 880 nm LED, LED stand, and micro-spectrometer, (C) LED Display, (D) Power switch, (E) Keypad.

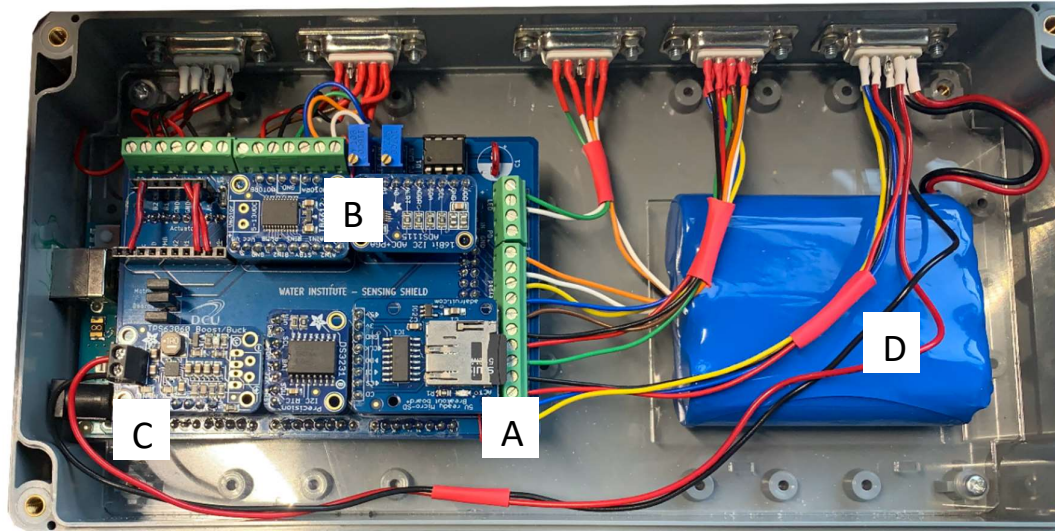


Figure 35: Layout of the inner components of the system. (A) SD card, (B) LED gamma/intensity adjustment, (C) Battery plug in/port, (D) Battery.

A2.2 LED screen options

The following section details the operation of each of the system's menus and their functions. For details on how to run a disc/sample, refer to Section A2.3 To access each menu, press the corresponding letter on the keypad to select the desired option.

Menus A – C enable various parameters of the system to be customized: the spin speed, spin duration, LED intensity, and the integration time.

To turn on the system, flip the power switch. The LED will light up and begin the initializing process. Once the SD card has been initialized, the main menu for the system will be displayed.

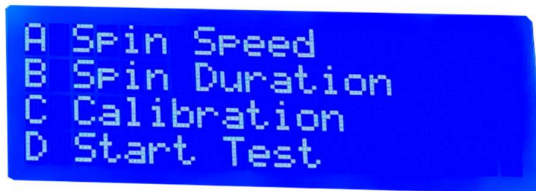


Figure 36: Main menu screen allowing access to various customization parameters and the analysis run program.

A2.2.1 Spin Speed Menu

The default programmed spin speed is 70 rotations per second (rps). If this value needs to be adjusted, press the *A* button on the keypad. This will open the spin speed menu (Figure 37). Here, the desired spin speed can be entered. Press # to save the input value and return to the main menu screen (Figure 36)

The entered value will be the default spin speed for any tests run until the system is turned off. If the system is turned off and back on again, it will return to the pre-programmed spin speed of 70 rps.

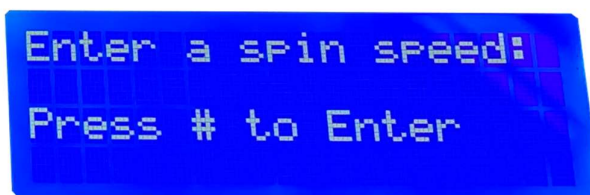


Figure 37: Spin speed menu

A2.2.2 Spin Duration Menu

The default spin duration is 30 seconds. If a different spin duration is desired, press the *B* button on the keypad and this will open the spin duration menu. Next, enter the

desired spin duration (in seconds) and press the # key. The system will then return to the main menu screen.

The entered value will be the default spin speed for any tests run until the system is turned off. If the system is turned off and back on again, it will return to the pre-programmed duration of 30 seconds.

A2.2.3 Calibration Menu

The C button opens the calibration menu (Figure 38). In this menu, two options will be available: Setting the Integration time (Section A2.2.4) and adjusting the LED intensity (Section A2.2.5). To return to the main menu, press the # key.

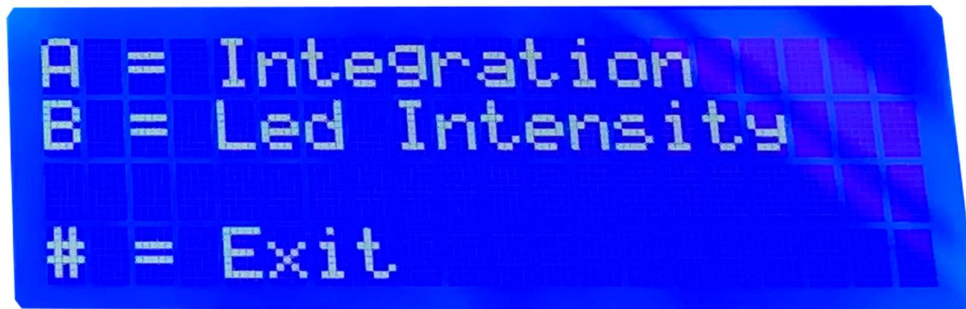


Figure 38: Calibration menu

A2.2.4 Integration menu

The default integration time is 0.0001 seconds. To adjust the integration time, press the A button in the calibration menu (Figure 38). Use the keypad to type in the desired integration time and then press #.

The entered value will be the default integration time for any tests run until the system is turned off. If the system is turned off and back on again, it will return to the pre-programmed time of 0.0001 seconds.



Figure 39: Integration time adjustment menu

A2.2.5 LED Intensity

Adjusting the LED intensity will require access to the control board of the system, which can be opened removing the system from its casing. Leaving the system powered on, a 3 mm hexwrench can be used to unfasten the screws securing the inner components to the metal frame of the system. A crosshead screwdriver can then be used to loosen the screws keeping the box holding the inner components secure and remove the lid. Next, mimicking Figure 40, slowly and gently turn the screw attached to the *LED gain* component of the control board with a flathead screwdriver. Turning the screw to the right will decrease the intensity and turning it left will increase the intensity.

To test the signal, open the LED intensity menu (Figure 41) by pressing the *B* button from the calibration menu. Press any key except for the *#* key and a reading of the light signal hitting the spectrometer will be taken and displayed on the screen. Continue to turn the

LED screw until the desired intensity is reached (just over 9,000 counts is ideal). Once the LED intensity is adjusted, press the # key to return to the calibration menu.

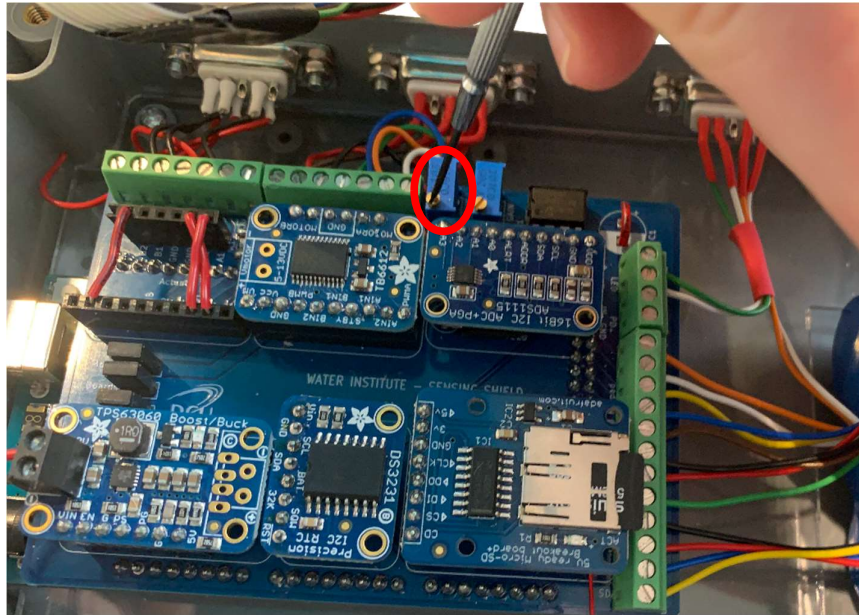


Figure 40: LED adjustment component

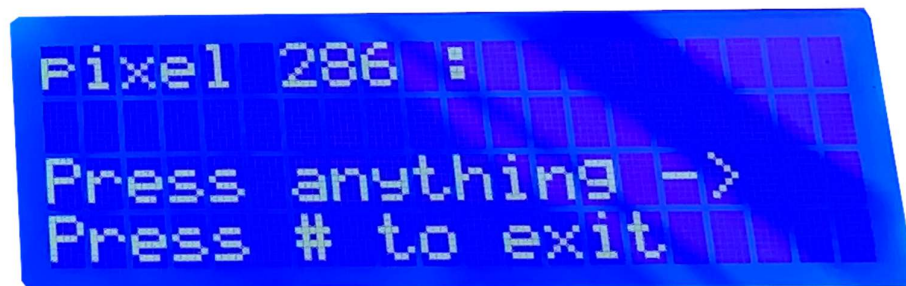


Figure 41: LED adjustment menu

A2.2.6 Start Test

The Start Test option (button *D*) will begin the testing sequence. Refer to Section A2.4 for further details.

A2.3 Analysing samples

A2.3.1 Preparing the Disc

A disc prepared with the necessary reagents for the molybdenum blue method pre-dried onto it, as described in Figure 26, is to be used. There are ten channels which can be used to analyse samples. For the purposes of this study, two channels were used for the analysis of premade standards, one for a control measurement of deionized water, and seven for field samples.

To analyse a sample, a syringe or Eppendorf pipette was used to inject 300 μL of sample into the reaction well. Fill the well until the entire well is filled and a tiny air pocket remains around the tip. Attach a 0.45 μm filter to the syringe or pipette to filter the sample before storage. This aids in preventing the micro-channels on the disc from clogging.

Once all of the samples have been added to the disc, gently shake the disc and wait 10 minutes for the reaction to take place. After the reaction is complete, the 2.5 mm hexwrench can be used to secure the disc to the spindle using the screws provided. For the system to be able to detect the channel location, it is crucial to make sure to line up the origin point (marked in Figure 42) with the arrow drawn on the spindle to make sure the analysis wells line up with the spectrometer and LED.



Figure 42: Aligning the disc with the spectrometer; * marks the origin point

A2.3.2 Sample Preparation and Deployment on Disc

The preparation required for field samples is to filter the sample through a 0.45 μm filter and then store the sample in a plastic, watertight container. For experiments shown in this document, a 15 mL centrifuge tube was utilized. This process is summarised in Figure 43.

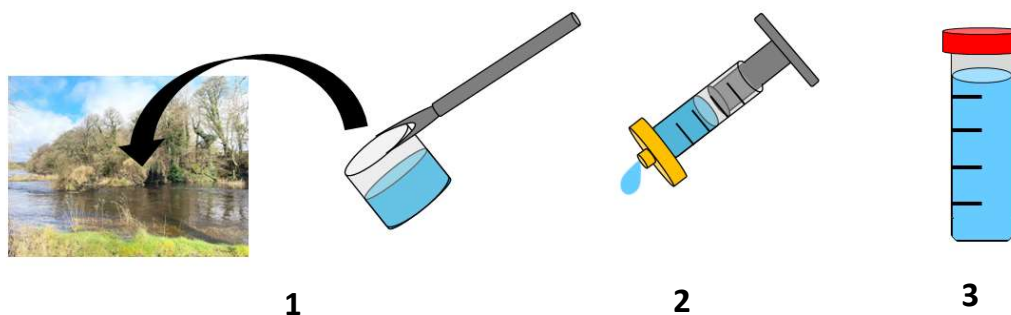


Figure 43: Field sample preparation steps for microfluidic analysis. (1) Collect the sample from the source. (2) Filter the sample using a 0.45 μm filter. (3) collect and

stored in a sample container before deploying onto the microfluidic disc. Store excess sample according to standardized guidelines²⁹.

After collection and filtration, samples can be deployed directly onto the disc using a micropipette or syringe. The sample is injected through the sample inlets shown in Figure 19, and 10 minutes are allotted for the sample to react with the combined reagents. Once the reaction is complete, the analysis program is run on the system (discussed in more detail in Chapter 3) and the results are displayed on the LCD screen on the system and stored on the SD card within the system for later analysis. Common settings for sample runtime are: spin speed = 60 rps, spin time = 30 seconds, integration time = 0.001 seconds.

Any excess sample which is collected and stored for later analysis must be kept in a cool environment and should be stable for approximately 48 hours²⁹.

A2.3.3 Running a Test

After the desired parameters were set (refer to Section A2.2 for setting system parameters), the *D* key on the main menu can be used to enter testing mode. The first screen displayed shows the integration time. If the integration time is incorrect, turn off the system for a few seconds and turn it back on. Then follow the instruction in Section A2.3.4 to reset the integration time.

Next, the system will prompt for the selection of the testing locations. Valid testing locations are listed as 0 – 9. 0 is the origin point and the reference the system uses to determine the location of the other 9 wells, which are 1 – 9 in the counterclockwise direction. Any combination of testing locations can be selected. It is important to note

that the first location tested will be treated as the blank and automatically subtracted from subsequent readings. The raw data for each reading is preserved in the saved data file (Section A2.4).

After the desired testing locations are selected, the # key will begin the test. If an error was made in the selection of the testing locations, the * key resets the selection.

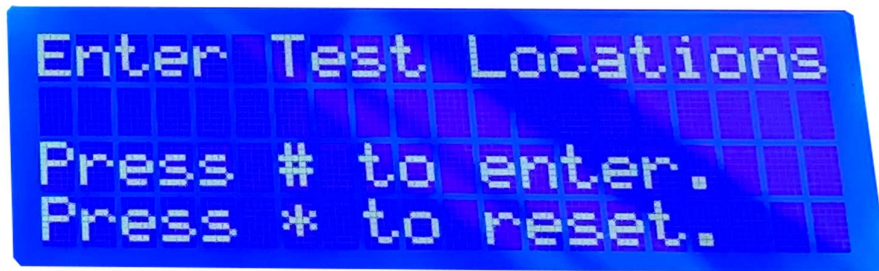


Figure 44: Testing locations menu

After the test starts, the motor will bring the spindle up to speed and then spin it for the desired spin duration. Once the spin sequence is complete, the system will decelerate and then move to the first testing location. After each reading, a series of screens will be displayed.

The first screen will display the default pixel read by the system, 286. This pixel corresponds to 880.4 nm in wavelength for this specific spectrometer model. Each model of the system will be slightly different with pixel to wavelength conversions, so it is necessary to double check the conversion chart provided by the manufacturer for the specific model being used. The other information displayed on this screen is the transmission counts recorded for the reading as well as the .TXT file name the data is saved under.

The second screen shows the raw reading of the sample directly compared to the raw reading from the blank at pixel 286 (880.4 nm).

The third screen shows the corrected transmission value for the sample with respect to the blank/first reading, as well as the absorbance reading.

After all of the readings are complete, the LED screen will return to the main menu.

A2.4 Data

A2.4.1 Extracting the Data

After the reading is complete, the data is saved on an SD card. To extract the data, open the box containing the inner components of the system as described in Section A2.2.5. The SD card should be gently pushed into its casing and then pulled out after a click is heard. The SD card should then be inserted into a computer/laptop and the data file copied from the SD card to the computer.

Files are saved under the following format: *day_month_hour.TXT* (Note: the system does not take into account daylight savings time. It is programmed under the GMT+1 time zone). If multiple tests are done in the space of a single hour, then all of the data will be saved in one file with the following heading separating each test within the file:

Test Carried Out: day/month/year - hour:minute - Integration time : 0.0001

The hour and minute listed is the time the analysis began.

A2.4.2 Analysing the Data

The data from the entire spectrometric reading for each well is saved in a single row of the .TXT file. Each row is labelled with the following:

Test well: #, 880nm Test Result: ____

Where ____ is the measured counts reading for the pixel 286 (880.4 nm).

Data can be converted from rows to columns using Excel's transpose feature if desired.

A2.5 Other System Customizations

A2.5.1 Adjusting the LED/Spectrometer Distance

If a custom disc is being used, the distance between the LED/spectrometer and the spindle can be adjusted if needed. To adjust the distance, the 4 screws highlighted in Figures 45 and 46 need loosened. Slide the holder to the desired location and re-tighten the screws. The ideal location is where the sensor of the spectrometer is in the centre of the analysis area of the disc. Make sure that the spectrometer is not pressed against the edge of the metal frame.

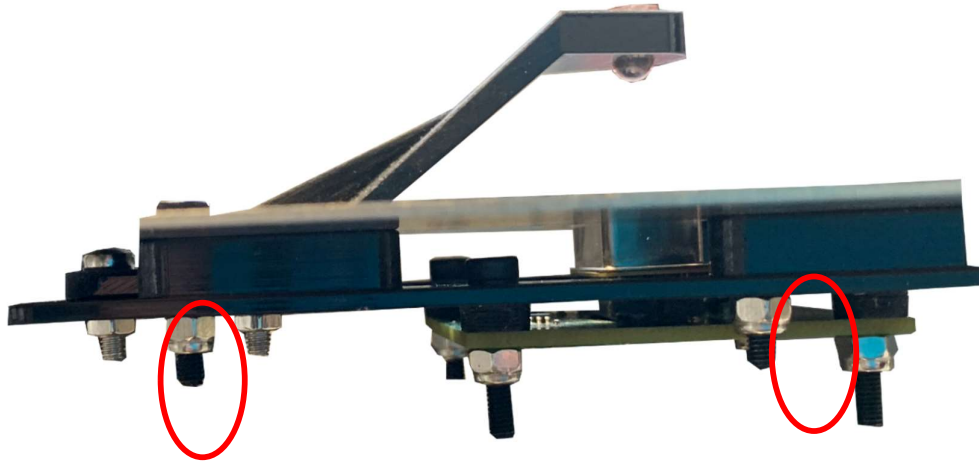


Figure 45: LED and spectrometer stage - side view; screws which need loosened to adjust the stage are highlighted.

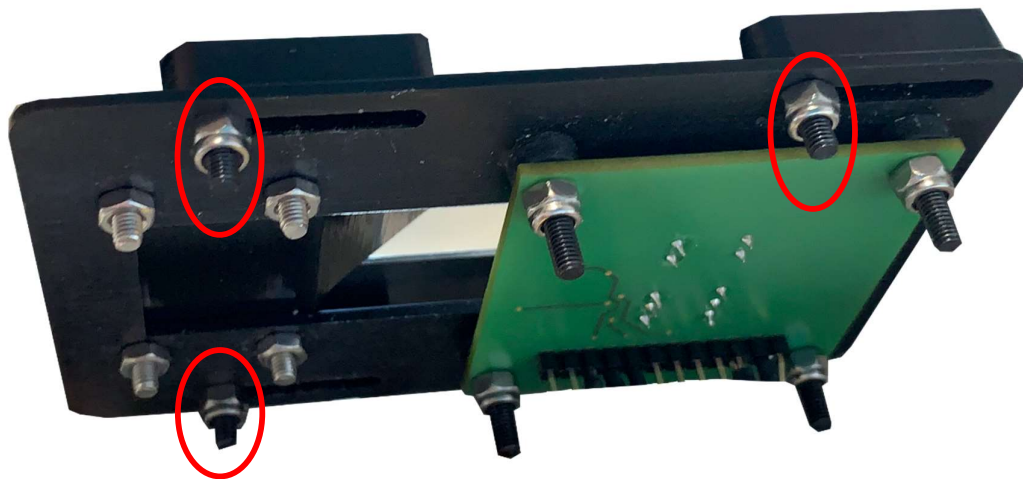


Figure 46: LED and spectrometer stage - bottom view; screws which need loosened to adjust the stage are highlighted.

A2.5.2 Charging the Battery

To charge the battery of the system, open the box containing the inner components of the system as described in Section A2.2.5. Using a 1.8 mm flathead screwdriver, loosen the screws securing the red and black wires to the battery component of the control board (highlighted in Figure 47).

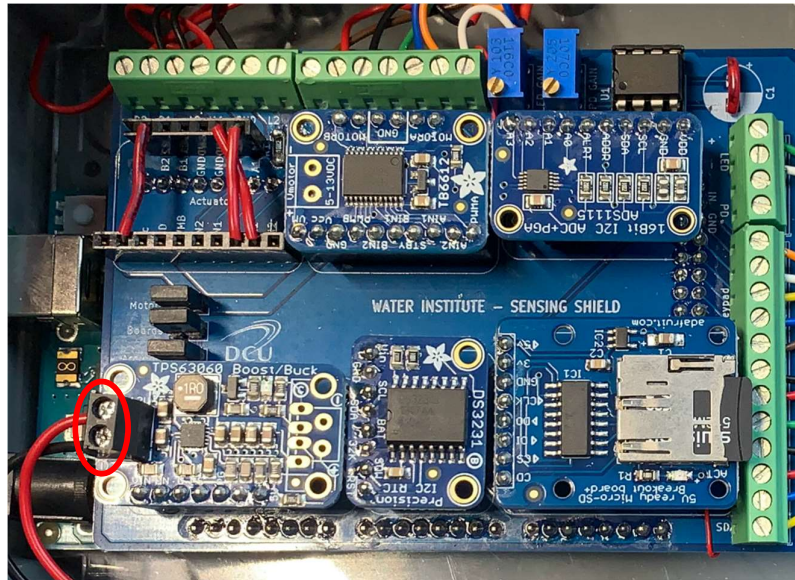


Figure 47: Control board of system - screws required to loosen for charging the battery are highlighted

The red and black wires should be secured to the custom charging board by tightening the screws on the custom charging board with the 1.8 m/m flathead screwdriver, red to positive and black to negative. Make sure the custom charging board is plugged into the charging unit. When ready to begin charging, flip the power button to the on position. A green light should be blinking on the charger plug. When the light is a steady green, the system is charged and the wires can be returned to their original placements on the system control board. Do not over charge the battery.